Summer 6-21-2018

Selective Muscle Degeneration in a Drosophila Model of Cachexia; A Role for the Transcriptional Regulator cabut

Matthew Giedd

Kennesaw State University
Graduate College

Thesis/Dissertation Defense Outcome

Name Matthew Giedd KSU ID 000342009

Email mgiedd@students.kennesaw.edu Phone Number 404-457-8496

Program MSIB

Title Selective muscle degeneration in a Drosophila model of cachexia; A role for the transcriptional regulator cabut

Thesis/Dissertation Defense: Date 6/21/18

[X] Passed [ ] Failed [ ] Passed With Revisions (attach revisions)

Signatures

Anton Bryantsev Thesis/Dissertation Chair	6/21/18 Date
Martin Hudson Committee Member	7/27/18 Date
[illegible] Committee Member	7/31/18 Date
Scott Nowak Committee Member	7/31/18 Date
Committee Member	Date
[illegible] Program Director	8/27/18 Date
Dawn Lynn Vogtsberger Department Chair	7/3/18 Date
Graduate Dean	Date

Last Modified 05/26/16

SELECTIVE MUSCLE DEGENERATION IN A *DROSOPHILA* MODEL OF CACHEXIA; A ROLE FOR THE TRANSCRIPTIONAL REGULATOR *CABUT*

by

Matthew Giedd

Submitted in partial fulfillment of the requirements for the Master of Science Degree in Integrative Biology

Thesis Advisor: Anton Bryantsev, Ph.D

Committee Members: Scott Nowak, Ph.D, Martin Hudson, Ph.D, Joel McNeal, Ph.D

Department of Molecular and Cellular Biology

Kennesaw State University

TABLE OF CONTENTS

ABSTRACT

Cachexia is a systemic metabolic syndrome characterized by progressive muscle wasting. Cachectic muscle wasting presents as a comorbidity with pathological illnesses like cancer, chronic inflammation, and type 2 diabetes. The development of cachexia complicates treatment of these diseases and worsens clinical outcomes. Thus, it has become the focus of intense investigation. While many of the upstream mechanisms that propagate cachectic muscle wasting have been brought to light, little is known of the downstream mechanisms which would be more clinically relevant. Here, we have adopted a *Drosophila* model of cachectic muscle wasting to elucidate a novel role of the transcriptional regulator, *cabut* (*cbt*), in selective degeneration of flight muscles over jump muscles. We report that *cbt* impairs mitochondrial function and expends vital glycogen stores from the flight muscles. Our results contend that the resilience of the jump muscles to degeneration resides in their low oxidative output and sporadic energetic requirements. Furthermore, we have implicated *cbt* as a positive regulator of jump muscle fiber number during muscle development.

INTRODUCTION

Cachexia is a lethal metabolic syndrome

Muscle wasting is a loss of muscle mass and function that manifests through atrophy (muscle fiber shrinkage) and fiber degeneration (fiber loss) (Bonaldo and Sandri 2013). The process of muscle wasting is a natural part of aging, but it can be accelerated through inactivity or disease. Cachexia is a metabolic syndrome characterized by progressive wasting of skeletal muscle (Langstein and Norton 1991). Cachectic muscle wasting is a collateral condition inducible by numerous pathological conditions such as cancer, chronic inflammation, congestive heart failure, and diabetes (Saitoh et al. 2017; Sayer et al. 2005). In many cases, cachexia becomes the primary cause of death. Sudden cardiac failure and respiratory failure (inability to support breathing due to weak diaphragm and intercostal muscles) comprise some of the most common causes of death in cachectic patients (Porporato 2016).

It is estimated that half of all cancer patients develop cachexia (Argilés et al. 2014). Strikingly, cachexia is attributed as the immediate cause of death in 20% to 40% of late-stage cancer patients (Fox et al. 2009). Like all cachectic conditions, cancer cachexia (simply, cachexia in the presence of a tumor) is complex and cannot be attributed to a single defect. Impaired cell signaling in pathways regulating inflammatory mechanisms, autophagy, nutrient response, glucose metabolism, proteostasis, and other physiological functions has been implicated in the development of cancer cachexia (Aoyagi et al. 2015). Since muscle wasting is largely responsible for the morbid effects of cachexia, there is a continuing interest from the research community to further reveal molecular mechanisms that make muscles sensitive to tumor presence (Zhou et al. 2010; Kir et al. 2016; Fukawa et al. 2016).

The insulin/insulin-like signaling pathway and its involvement in muscle wasting

There is reason to believe that dysregulated insulin/insulin-like growth factor-1 (IGF-1) signaling (IIS) has a major role in the pathogenesis of cancer cachexia (Lundholm et al. 1978; Costelli et al. 2006). Insulin and IGF-1 belong to heavily conserved evolutionary lineages of peptide hormones (Pertseva and Shpakov 2002). The most well-known function of insulin is to regulate systemic glucose homeostasis by both stimulating glucose uptake by cells and suppressing glucose synthesis in the liver (Weiss et al. 2014). A less appreciated, but equally vital function of insulin is to promote protein synthesis and inhibit protein degradation in muscles (Meek et al. 1998). IGF-1 regulates muscle proteostasis in similar anticatabolic fashion (Goldspink 1999). *In vivo* experiments in rodents have demonstrated hypertrophic effects of IGF-1, and *in vitro* studies found that IGF-1 promotes human myotube hypertrophy in cell cultures (Barton-Davis et al. 1998; Jacquemin et al. 2004). In mice, insulin receptor (IR) knockdown causes skeletal muscle wasting, likely due to atrophy caused by reduced protein synthesis. (O'Neill et al. 2010). Clearly, the IIS pathway has critical roles in metabolism and muscle mass maintenance that, if disrupted, could lead to cachectic muscle wasting.

Effectors of the insulin/insulin-like signaling pathway in muscle wasting

There has been considerable effort to resolve the molecular mechanisms downstream of IIS that lead to cachexia. Insulin/IGF-1 binding to IR and IGF1R induces similar downstream signals through the PI3K/Akt and MAPK pathways (Belfiore et al. 2009; Boucher et al. 2014). Activated PI3K phosphorylates the Ser/Thr kinase, Akt, which can then suppress nuclear translocation of Forkhead box O (FoxO) transcription factors through inhibitory phosphorylation events. FoxO is the main activator of gene expression under negative regulation by IIS. FoxO transcription factors induce expression of muscle-specific E3 ubiquitin ligases which mediate muscle atrophy by conjugating ubiquitin to protein substrates, thereby targeting them for degradation in the proteasome (Sandri et al. 2004; Stitt et al. 2004; Bodine et al. 2001a). Thus,

when IIS is suppressed, FoxO may contribute to cachectic muscle wasting through enhancement of protein degradation. Indeed, expression of *FOXO1* in transgenic mice was shown to reduce skeletal muscle mass. Moreover, these mice had reduced capacity for glucose metabolism and reduced quantities of red muscle fibers (Kamei et al. 2004).

Akt can also induce activity of the mechanistic target of rapamycin (mTOR). The most well described function of mTOR is to negatively regulate the eukaryotic translation initiation factor 4E (eIF4E)-binding protein 1 (4E-BP1). 4E-BP1 is thought to repress protein synthesis by binding eIF4E, thereby preventing eIF4E from associating with its translational complex (Gingras et al. 1998). Evidence suggests that mTOR dissociates the inhibitory complex through phosphorylation of 4E-BP1 at multiple sites (Gingras et al. 2001). In mice, it was shown that Akt/mTOR activation could suppress atrophy, supposedly by preventing eIF4E-4E-BP1 complex formation (Bodine et al. 2001b). Surprisingly, studies have shown that overexpression of the 4E-BP1 *Drosophila* homolog, *Thor*, delays age-related muscle wasting (Demontis and Perrimon 2010). Furthermore, *Thor* has an apparent role in starvation and oxidative stress resistance by enhancing mitochondrial activity (Zid et al. 2009; Tettweiler et al. 2005; Teleman et al. 2005).

There is some debate that stimulation of IIS and Akt/mTOR signaling can directly inactivate 4E-BP1. One study found that increased insulin sensitivity in mice was correlated with an upregulation of ubiquitin-proteasome system components but did not increase expression of 4E-BP1 and other factors involved in protein synthesis (dos Santos et al. 2016). Stimulation of inflammatory pathways and expression of cytokines like tumor necrosis factor-alpha (TNF-α) has been shown to repress protein synthesis by dissociating the eIF4E translational complex, suggesting that pathways other than IIS control translation (Tisdale 2008).

Muscle wasting is one of many numerous physiological changes that can be traced to aberrant function of the IIS pathway. The broad range of downstream transcriptional targets

responsible for such changes remain poorly defined, despite better understanding of upstream signal transduction. As such, there is a distinct need to determine what effector molecules mediate cachectic wasting.

Disrupted carbohydrate metabolism is a hallmark of cachexia in cancer and Type 2 Diabetes (T2D), another disease in which cachexia commonly manifests. This disruption encompasses hyperglycemia, high endogenous sugar production (particularly from amino acids) and enhanced anaerobic recycling of glucose (Chevalier and Farsijani 2013). Given the pervasiveness of carbohydrate metabolism dysregulation in these diseases, it is plausible that participant genes in this regulation may be driving cachectic muscle wasting.

Emerging evidence implicates the Krüppel-like Factor (KLF) family of transcription factors in carbohydrate metabolism – and possibly muscle wasting. Recently it was shown that glucocorticoids, a class of hormones that regulate glucose homeostasis, can induce muscle wasting by activating KLF15. Two other members of this family, KLF10 and KLF11, are notably upregulated in pancreatic and intestinal cancers, which are highly associated with cachexia (Tetreault et al. 2013; Tisdale 2002). KLF10 is thought to respond to increased glucose by broadly altering metabolic gene expression, in a mechanism interlinked with circadian rhythm (Guillaumond et al. 2010). Conversely, KLF11 is believed to bind the insulin promoter in a compensatory response to low intracellular glucose (Zhang et al. 2013). Altogether, these studies suggest a critical function of KLFs in regulating glucose homeostasis, although investigation into their role in muscle wasting has just begun.

The mechanisms regulating carbohydrates are remarkably conserved in vertebrates and invertebrates. For example, functions closely resembling those of KLF10 and KLF11 have been ascribed to their *Drosophila* homolog, *cabut* (*cbt*) (Bartok et al. 2015; Havula et al. 2013). Due to such similarities, in addition to ease of use, *Drosophila* has gained significant traction as a

model to study carbohydrate metabolism (Mattila and Hietakangas 2017). For example, knockdown of insulin-like peptides in *Drosophila* has proved to be a useful tool in modeling type 2 diabetes (Murillo-Maldonado et al. 2011). Since altered carbohydrate metabolism is commonly observed in cachectic patients, broader investigations into such phenomena may shed light on the molecular mechanisms driving cachexia.

Heterologous composition of skeletal muscle

To begin identifying molecular mechanisms of cachexia, some understanding of the heterogeneous nature of mammalian muscle is necessary. In mammals, skeletal muscle is comprised of several fiber types whose ratios determine the overall functional output (Scott et al. 2001). These fiber types differ in metabolic profiles, mitochondrial content, structural gene expression, and contractile properties (Bottinelli and Reggiani 2000). Human skeletal muscle fiber types can be categorized as slow-twitch (Type I) or fast-twitch (Type IIa or Type IIx). Slow-twitch fibers are characterized by high oxidative capacity and low force generation, but robust fatigue resistance. As such, greater proportions of slow-twitch fibers are ideal for endurance activities. Type IIa (oxidative-glycolytic) fibers parallel slow-twitch fibers in oxidative capacity, but use more readily metabolized energy sources, produce greater force, but become exhausted faster. Lastly, Type IIx fibers (fast glycolytic) are quickest to fatigue but yield the highest force, making them most suitable for short bursts of activity. Different muscles in the body are naturally predisposed to certain proportions of fiber types (Pette and Staron 2000). The soleus muscle of the lower leg, for example, is involved in long-term activities like posture support and walking. As such, high density of slow-twitch fibers is intrinsic to the soleus muscle. Variant muscle-to-muscle ratios of Type I and Type II fibers, which have distinct metabolic requirements, could mean that certain muscle groups are more susceptible to cachectic muscle wasting than others.

Nevertheless, muscle fiber ratios in mammals are not static but highly plastic with age, diet, and exercise, or lack thereof (Pette and Staron 2000). This implies that fiber ratio fluctuates to accommodate different physiological demands. Indeed, muscle biopsies of elite athletes illustrate the adaptiveness of human skeletal muscle. In one champion sprint runner, biopsies revealed that Type IIx fibers were far more abundant than normal individuals. Moreover, the capacity of the runner's Type IIx fibers to generate power eclipsed that of both untrained individuals and other high-level performing athletes from different disciplines (e.g. distance runners, competitive swimmers) (Trappe et al. 2015). Interestingly, fast glycolytic fibers, which can more rapidly and efficiently utilize glucose and other metabolites than their oxidative counterparts (Type I and IIa), may be more resistant to the negative effects of insulin resistance and type 2 Diabetes (LeBrasseur et al. 2010). At the other end of the spectrum, efficiency of cycling, an endurance activity, is positively correlated with greater percentages of Type I fibers (Coyle et al. 1992). These data highlight the dynamic nature of skeletal muscle fibers, but also extend the possibility that cachectic pathology may affect muscle fibers differently.

Drosophila as a model for muscle wasting

In many respects, the metabolic profiles and structural organization of *Drosophila* and human muscles are analogous, and therefore suitable for comparative studies of muscle wasting. The largest muscles in *Drosophila*, the indirect flight muscles (IFMs) and the tergal depressor of the trochanter (TDT, or jump muscle), have specialized functions based on their constituent fiber type (fibrillar and tubular, respectively). Flight muscles are outfitted with large quantities of mitochondria and glycogen to continuously power extended bouts of flight. Correspondingly, tubular-type jump muscles, which are used less frequently, are less densely packed with mitochondria and glycogen (Deak 1977). These muscles can be further classified by differential expression of constitutive genes within them (Oas et al. 2014; Bryantsev et al.

2012a). Thus, the diversity of fiber types in *Drosophila* makes it a suitable model system to study cachectic muscle wasting.

Drosophila is a genetically tractable model organism. One of the best examples of this is the GAL4/UAS expression system. In the binary GAL4/UAS system, the yeast transcriptional activator GAL4 is inserted under the control of a native genomic enhancer in one parental stock. In the other stock, the upstream activated sequence (UAS), another genetic element exported from yeast, is strategically placed upstream of genes of interest. Offspring of these parents will express GAL4 corresponding to the activity of the endogenous enhancer (i.e. if the enhancer is active in a specific tissue or developmental timepoint, GAL4 will exclusively be expressed there). Expressed GAL4 then specifically binds to the UAS, promoting transcription of the gene of interest (Brand and Perrimon 1993). For targeted gene downregulation, UAS-controlled, inverted-repeat constructs are expressed. Upon transcription, these constructs collapse to produce double-stranded RNA molecules that match the sequence of targeted mRNA transcripts and work to eliminate those transcripts via the phenomenon of RNA interference (Wilson and Doudna 2013).

A GAL4/UAS model for cachexia-like muscle wasting was recently published (Kwon et al. 2015). In this model, *yorkie* (*yki*), a transcriptional coactivator that regulates cell proliferation and growth, was overexpressed in the fly midgut using the *escargot* (*esg*) GAL4 driver, which is active specifically in intestinal stem cells. This yielded uncontrolled cell proliferation within the fly midgut and induced wasting of peripheral tissues (fat body, ovary, muscles). Importantly, to bypass lethality in larvae, the GAL4/UAS system was modulated with a temperature-sensitive construct that made tumor growth permissible only at higher temperatures (Suster et al. 2004). In addition to systemic wasting, genes involving energy metabolism were broadly repressed in the muscles of tumor-bearing flies. Notably, IIS pathway components were downregulated in those muscles.

Here, we employ the same tumor-bearing flies (hereafter *esg>yki*^{act}) to examine the molecular mechanisms of cachectic muscle wasting. We aimed not only to identify novel factors mediating muscle wasting, but also to evaluate whether certain fiber types, due to their metabolic differences, are more susceptible to muscle wasting.

RESULTS

Midgut tumors affect muscle performance

We induced cachexia-like wasting in flies through the inducible *esg>yki*^{act} system (Fig. 1A). In *esg>yki*^{act} flies, tumor growth is made temperature sensitive through repression of the GAL4/UAS system at 18°C, but can be induced by switching newly emerged adult flies to warmer conditions at 29°C. When neoplasia is induced, *esg>yki*^{act} tumor-bearing flies undergo dramatic fat body and muscle wasting (Kwon et al. 2015). We observed that temperature-activated *esg>yki*^{act} flies have significantly shorter lifespans than controls, with the majority dying within the first 2 weeks of life. Based on this observation, we used 2-week old flies in most of our tests.

We sought to further characterize the possible impact of the midgut tumor on the functionality of the indirect flight muscles (IFMs) and the tergal depressor of the trochanter (TDT or jump muscle). IFMs solely generate power to propel wings during flight (Lindsay et al. 2017) and, therefore, their functional state can be directly inferred from a test for upward flying mobility. Similarly, TDTs are exclusively responsible for jumping action, and their functional state can be determined by measuring average jumping distance.

Cachectic *esg>yki*^{act} flies progressively lost flying ability as they aged. After two weeks of tumor growth, only 34% of *esg>yki*^{act} flies were able to fly ($p<0.01$, see two-proportion z-tests in Table 1), whereas 90% of age-matched control flies retained flying ability (Fig. 1C). In contrast, TDTs did not demonstrate exacerbated functional decline, retaining 80% of the initial jumping power at two weeks in *esg>yki*^{act} flies (Fig. 1D). Our results confirm that experimentally induced tumor-like growth in the fly midgut induces cachexia and specifically impairs the functional state of somatic muscles. Notably, IFMs and TDTs have different response rates, the former being most sensitive to the tumor presence.

Flight and jump muscles respond differently to tumor presence

To gain insight into the functional differences observed for , we evaluated biochemical differences between these two muscle types. IFMs are very energetically active due to their demanding functional role to power flight, which is reflected by high mitochondrial content and stored glycogen levels (Deak 1977). We tested mitochondrial function with an enzymatic assay of succinate dehydrogenase (SDH) activity (Pearse 1972). SDH is a protein complex located within the inner mitochondrial membrane which plays key roles in both the citric acid cycle and electron transport chain (Hederstedt and Rutberg 1981). In this assay, both control and young *esg>yki*^{act} flies, before tumor induction, have IFMs that are strongly positive for SDH activity. In stark contrast, TDTs, which become activated for contractions only occasionally, are negative for SDH activity and glycogen (Fig. 2A, D). After two weeks, *esg>yki*^{act} flies displayed SDH-negative IFM fibers (Fig. 2A). The lack of SDH activity is indicative of dysfunctional mitochondria and ultimately results in fiber degeneration. Indeed, additional examination of SDH-negative fibers often revealed signs of fiber integrity breaches, picnotic nuclei, and alterations in myofibrilar striation pattern (not shown). The SDH assay revealed that approximately 27% of IFM fibers from two-week old *esg>yki*^{act} flies lacked functional mitochondria (Fig. 2B). The occurrence rate of IFM degeneration was high, as we observed degenerate fibers (i.e., at least one degenerate fiber) in 37% of two-week old *esg>yki*^{act} flies ($p<0.05$, see two-proportion z-tests in Table 2), but no degeneration was observed in the control group (Fig. 2C).

IFMs store large quantities of metabolically available glucose in the form of glycogen to power extended periods of flight (Sacktor 1955). We hypothesized that glycogen loss could be responsible for impaired mitochondrial function in *esg>yki*^{act} flies. In two-week old *esg>yki*^{act} flies, 46% of fibers assessed lacked glycogen. We observed glycogen loss in 10% of fibers in two-week old control flies (Fig. 2E). Incidence of glycogen depletion was evident, as 60% of two-week old *esg>yki*^{act} flies ($p<0.05$, Table 2) showed signs of glycogen loss, compared to only

20% of control flies (Fig 2F). Where one fiber was glycogen-deficient in *esg>yki*^{act} IFMs, the remaining fibers were similarly lacking glycogen in the same fly.

Unlike IFMs, TDTs store very little glycogen (Deak 1977). Interestingly, in the cases of total glycogen loss in IFMs of two-week old *esg>yki*^{act} flies, we observed unusual accumulation of glycogen within TDTs (Fig. 2D). This observation serves as another remarkable indication that IFMs and TDTs have different responses to tumor presence. Our data suggest that IFMs undergo metabolic changes, resulting in depletion of glycogen stores, which might trigger mitochondrial damage and subsequent death of IFM fibers.

Since TDTs do not demonstrate readily detectable SDH activity, we analyzed another marker of muscle degeneration – loss of staining for polymerized actin (F-actin), a major component of the contractile apparatus. For this, we probed for the absence of F-actin in TDT fibers. To confirm that regions lacking F-actin were indeed once fibers, we only counted those regions in which cell membranes could be visualized (Fig. 3A). Impressively, less than 1% of TDT fibers in both two-week old control and *esg>yki*^{act} flies were ranked as degenerate (Fig. 3B). Of the flies assessed, we observed at least one degenerate fiber in 13% of control flies and 21% of *esg>yki*^{act} flies (Fig. 3C). Since F-actin assessment can only account for fibers that are in the process of dying, we also searched for changes in the numbers of live TDT fibers (since *Drosophila* muscles are naturally lacking regeneration mechanisms). When comparing the median numbers of counted fibers between control and *esg>yki*^{act} flies, we did not observe any significant difference (Fig. 3D). These results, in contrast with IFM data, support the notion that TDTs are less susceptible to the effects of the experimental gut tumors.

Altogether, our data demonstrate that the basis for differential functional response of IFMs and TDTs to tumors in cachectic flies can be in the pronounced difference in energy

demands. Another potential factor could be in the intrinsic, fiber-specific differences in carbohydrate control, characteristic of each of these muscles.

Transcriptional changes in muscles of cachectic flies

To determine molecular factors that might mediate muscle degeneration in *esg>yki^{act}* flies, we analyzed whole-transcriptome changes in IFMs and TDTs collected one week after experimental tumor onset, at the midpoint of degenerate IFM fiber development. Total RNA extracted from dissected IFMs and TDTs was submitted for next-generation sequencing. Overall, the amount of total RNA extracted from IFMs was relatively low, but the relative abundance of transcripts in those samples was maintained as expected, meaning genes with well-known expression profiles maintained those profiles (not shown). This includes muscle structural genes, such as actin and myosin heavy chain, as well as mitochondrial and metabolic genes involved in glycolysis and respiration. To better visualize the relevant expression levels between IFMs and TDT muscles, we normalized expression of each gene by the levels of *Mef2*, a pan-muscular gene that is moderately expressed from the early stages of muscle development and throughout adulthood (Bour et al. 1995; Bryantsev et al. 2012a). Muscles from one-week old control and *esg>yki^{act}* flies were analyzed in parallel.

Next, we used RNAseq data to identify critical regulators that might be responsible for IFM sensitivity to tumor presence. We selected two candidate genes, *cabut* (*cbt*) *and Thor*, whose expression elevated in the presence of experimental tumors (Fig. 4A). Endpoint PCR also confirmed the expressional changes of our genes of interest in *esg>yki^{act}* flies (Fig. 4B). We selected both genes based on their conserved sequences and function in humans. Reiterating, *Thor* is strictly conserved across all eukaryotes and plays a central role, downstream of IIS, in regulating translation initiation (Gingras et al. 1999). Most similar to *cbt* are the Krüppel-like factor (KLF) proteins KLF10 and KLF11 (Muñoz-Descalzo et al. 2007), which both have roles in glucose sensing mechanisms (Bartok et al. 2015).

Effects of *cbt* and *Thor* overexpression in flight muscles

To explore the role of *cbt* and *Thor* in muscle degeneration, we overexpressed *cbt* and *Thor* with the GAL4 driver under the control of the *flightin* (*fln*) enhancer (Bryantsev et al. 2012b). Critically, *fln* expression is robust and localized exclusively to the IFMs, where it is required for myosin thick filament assembly (Fig. 5A) (Reedy et al. 2000). Expression of *fln* begins in the late pupal stages and continues throughout adulthood, although its expression weakens with age (Vigoreaux et al. 1993). We first evaluated the functional impact of *cbt* or *Thor* overexpression on IFMs. For this, we drove expression of wild-type *cbt* and a consitutively active *Thor*, mutated at a key regulatory phosphosite. Strikingly, *fln>cbt* adults were entirely unable to fly, from the youngest age ($p<0.01$, Table 1), which suggested that *cbt* has an impact on IFM physiology. In contrast, 75.3% of *fln>Thor*^{act} flies ($p=0.14$, Table 1) retained flying ability at two weeks old (Fig. 5B). Given the dramatic functional loss observed in IFMs, we selected *cbt* for further analysis.

cbt overexpression induces morphological and biochemical changes in flight muscles similar to those observed in cachectic flies

Based on the flight test results, we strongly suspected that the IFMs of *fln>cbt* flies would have extensive mitochondrial dysfunction and glycogen depletion. In two-day old *fln>cbt* flies, 0.5% of IFM fibers were degenerate. After two weeks, the proportion of degenerate IFM fibers substantially increased to 38.8%, mirroring the rate of fiber degeneration observed in *esg>yki*^{act} flies (Fig. 6B). However, 90% of two-week old *fln>cbt* flies ($p<0.01$, Table 2) showed some signs of degeneration, greatly surpassing the incidence seen in *esg>yki*^{act} flies (Fig. 6C).

Impressively, glycogen stores in two-day old *fln>cbt* flies were completely depleted, while all IFM fibers of the control group had glycogen. By two weeks, only 6.1% of IFM fibers of control flies lacked glycogen. We observed that 22.9% of IFM fibers of two-week old *fln>cbt* flies had returned to normal glycogen levels (Fig. 6E). The most likely explanation for this modest

recovery is that *fln*-GAL4 expression, which drivers *cbt* expression in this system, weakens with age. The gradual dampening of *cbt* levels would allow for some IFM fibers to return to normal metabolic conditions. Despite this, we still observed glycogen-deficient fibers in 100% of *fln>cbt* flies, both at two-days and two-weeks old (Fig. 6F) ($p<0.01$ and $p<0.05$, respectively; Table 2). We observed incidences of glycogen loss in 73.3% of two-week old control flies. It is well known that glycogen levels diminish following activity, or increase after eating (Deak 1977). The high incidence of glycogen loss in control flies is likely due to this innate variability in glycogen levels.

These results indicate that targeted overexpression of *cbt* within the IFMs has dramatic effects on the ability to retain vital glycogen stores. While the magnitude and prevalence of SDH activity loss and glycogen loss is more pronounced in *fln>cbt* flies, these results point to a shared condition of a metabolic dysregulation within the IFMs of *esg>yki*^{act} and *fln>cbt* flies, coinciding with increased rates of muscle fiber degeneration.

Characteristic morphological changes of cachectic and *cbt*-overexpressing flight muscles

Thus far we have shown that the IFMs of *esg>yki*^{act} flies and *fln>cbt* flies suffer similar loss of functionality, mitochondrial activity, and glycogen content. In addition to this, SDH analysis revealed a unique morphological feature that was shared by both experimental groups – distinct perforations throughout IFMs (Fig. 7A, 7D). We saw perforations only in IFMs – typically before the onset of the massive fiber degeneration. Perforations were usually observed in one-week old *esg>yki*^{act} flies, while they were more frequently observed in two-day old *fln>cbt* flies. The unique nature of the perforated phenotype strongly links the deleterious effects of *cbt* overexpression to the muscle degeneration seen in *esg>yki*^{act} flies. Despite this, the exact nature of this phenomenon is unknown.

We attempted to further characterize the perforations by assessing both the mitochondria and t-tubules of *esg>yki*^{act} flies. Streptavidin (marker for mitochondrial content)

staining did not show any discernible mitochondria loss, nor did α-dlg staining show t-tubule presence within the perforations (Fig. 7B, 7C). Furthermore, we probed for the formation of poly-ubiquitin aggregates, a sign of heightened autophagy (Morimoto et al. 2015), but we did not observe any aggregates in control or *esg>yki*^{act} flies (not shown). Higher resolution analysis with electron microscopy will be performed to confirm the nature of the damage where these methods could not, in addition to highlighting the similarities and differences between the perforations of *esg>yki*^{act} and *fln>cbt* flies. Since neither t-tubules nor mitochondria are present in the perforations, we propose that accumulation of excess water into the cytosol may be the causitive factor.

cbt overexpression does not harm jump muscles, and a possible role of *cbt* in jump muscle fiber specification

Our next step was to characterize the effects of *cbt* overexpression on TDTs. To do this, we used the GAL4 driver made with the enhancer elements of muscle-specific gene *Actin 79B* (*Act79B*-GAL4), which is active in TDTs, but not IFMs (Bryantsev et al. 2012a). Like *fln*-GAL4, *Act79B*-GAL4 expression begins in the late stages of muscle development and persists throughout adulthood (Fyrberg et al. 1983). To our surprise, overexpression of *cbt* in TDTs was not deleterious, but resulted in extensive muscle hypertrophy (Fig. 8A). When compared to control flies, the average fiber number and surface area of *Act79B>cbt* flies increased by 58.7% and 56.3%, respectively (Fig. 8B). At the same time, we did not observe any significant difference in jumping ability between *Act79B>cbt* and control flies (Fig. 8C). TDTs respond in an altogether different manner to *cbt* overexpression than IFMs. Therefore, it is possible that *cbt* is part of the molecular mechanism controlling selective response of different muscle types (flight, jump) to tumor presence. Furthermore, *cbt* appears to regulate TDT fiber number.

cbt induces its deleterious effects independent of the insulin pathway

Currently, the regulatory mechanisms controlling the *cbt* gene are poorly understood. Therefore, we wanted to find a place for *cbt* within the cell signaling network of the IFMs. The most immediate candidate for testing was the IIS pathway. Given the well-established role of IIS in muscle mass maintenance (Meek et al. 1998; Goldspink 1999) and the putative role of IIS dysregulation in the cachectic phenotype of *esg>yki*^{act} flies (Kwon et al. 2015), we decided to probe the effects of IIS suppression on IFMs. For that, we overexpressed a dominant-negative K1409A mutant of the insulin receptor (*InR*) that lacked tyrosine kinase activity with the GAL4 *fln* driver. Only 46.2% of *fln>InR*^{DN} flies were capable of upward flying at two days old, and by two weeks, all were unable to fly (Fig. 9A) ($p<0.01$ at both timepoints, Table 1). As expected, IIS suppression had harmful effects on mitochondrial function and glycogen storage in IFMs. Surprisingly, however, mitochondrial damage was substantially less pronounced than those caused by the midgut tumor in *esg>yki*^{act} flies. In two-week old *fln>InR*^{DN} flies, only 6.8% of fibers fell under the degenerate category (Fig. 9B). Despite this, we observed significant glycogen loss in *fln>InR*^{DN} flies, which supports the notion that the IIS pathway was indeed repressed in these flies. In two-day old *fln>InR*^{DN} flies, 46.9% of IFM fibers were glycogen-deficient, but by two weeks glycogen levels had recovered to 18.8% (Fig. 9D). Again, this is likely due to diminishing *fln*-GAL4 expression as the flies age.

Since we did observe significant functional impairment and morphological damage as a result of IIS suppression, we proceeded with molecular analysis. To do this, we extracted RNA from the IFMs of *fln>InR DN* and *fln>cbt* flies and compared the effects on both *cbt* and *Thor* expression. *Thor* is typically repressed when IIS is active (Gingras et al. 1998). Accordingly, *Thor* expression increased in *fln>InR*^{DN} flies. Interestingly, *Thor* was upregulated in *fln>cbt* flies, but we did not see any induction of *cbt* in *fln>InR*^{DN} flies (Fig. 10A). These results place *cbt* as a

genetic activator of *Thor*, but the nature of the regulation (direct or indirect) is unclear. Moreover, activation of *cbt* itself does not seem to depend on the IIS pathway (Fig. 10B).

Surveying the transcriptome of *cbt*-overexpressing flight muscles for potential effectors of muscle wasting

Having characterized the deleterious effects of *cbt* on IFMs, we sought to identify commonly regulated genes between *esg>yki*^{act} and *fln>cbt* flies. Particularly, we were interested in genes that might regulate energy metabolism, given the extensive glycogen loss observed in both groups. For this, we extracted RNA from the IFMs of one-week old control and *fln>cbt* flies for next generation sequencing. We then analyzed annotations of genes that had significantly altered expression in both *esg>yki*^{act} and *fln>cbt* flies. Our analysis found no specific enrichment in genes of a particular function or process in *esg>yki*^{act} flies. Nonetheless, we found that genes associated with mitochondrial ATP synthesis were among those with the most significant presence in *fln>cbt* flies. We also observed upregulation of 6 genes involved in synthesis of carbohydrate derivatives (Table 3).

Since the enrichment analysis was limited, we again normalized our results to the expression of *Mef2* and compared the expression across all groups. A small set of candidate genes was manually extracted from this data (Table 4). The first of these candidates, *Cyp4p3*, an oxidoreductase, was commonly upregulated. It is suggested that oxidoreductases, which are the primary generators of reactive oxygen species, may drive oxidative stress in mitochondria (Kussmaul and Hirst 2006). Interestingly, *TotA*, a gene that has a putitive role in oxidative stress response, was downregulated (Ekengren et al. 2001). Finally, we determined that *target of brain insulin* (*tobi*), an O-glycosyl hydrolase, was upregulated. Glycosyl hydrolases are critical for enzymatic breakdown of polysaccharides such as glycogen (Davies and Henrissat 2015). Future work will evaluate whether aberrant expression of these genes can sufficiently induce degeneration of IFMs or rescue *cbt*-mediated IFM wasting.

DISCUSSION

In this study, we show that *yki*-driven midgut neoplasia impairs somatic muscle function and causes muscle fiber degeneration. While some of our data strengthen previously reported results (Kwon et al. 2015), we further describe selectivity in functional impairment of indirect flight muscles (IFMs) over the jump muscles (TDTs). Why would these two muscle types respond differently to tumor presence? We think that the reason lies in the difference of metabolic activity characteristic for these muscles. IFMs, like type I muscle fibers in humans, depend on oxidative phosphorylation for their main source of energy. This is evident by high density of mitochondria and high levels of SDH activity. In contrast, TDT muscle contains few mitochondria and low SDH activity. The downside of high mitochondrial content seems to be the constant high demand for oxidative phosphorylation substrates (e.g. glucose, fatty acids), even during periods of rest when no active work is being done. The high resource expenses could be a decisive factor driving muscle size reduction seen in mammals and humans upon fasting or prolonged muscle disuse (Hikida et al. 1989; Bouché et al. 2004). Mammalian fibers are highly plastic and can undergo reversible size reduction known as atrophy, but under chronic conditions the overall number of highly oxidative fibers in skeletal muscles dwindles. For example, fewer Type I fibers can be seen in diabetic patients and animal models of diabetes (Oberach et al. 2006; Song et al. 1999). Fiber-type specific atrophy has been also reported in response to cancer, but the type of responding fibers depends on specifics of cancer etiology. Usually, less oxidative Type II fibers are reported to atrophy in cancer patients (Mendell and Engel 1971; Acharyya et al. 2005).

In our fly model, instead of fiber atrophy we readily detect a more severe and irreversible response – fiber degeneration (i.e. death). This is because *Drosophila* skeletal muscles lack the regenerative capacity and plasticity of mammalian muscles. Within the scope of our model, this

fact comes as a strong advantage, since without repair we receive a faithful, quantifiable record of muscle response to an experimental condition. Fiber degeneration is a more common process in mammalian muscles undergoing atrophy, but it becomes significantly masked by an ongoing regeneration process that involves satellite cells (Borisov et al. 2001). Damage and elimination of oxidative capacity in IFMs is reminiscent of the disappearance of type I fibers during diabetes (Oberach et al. 2006). Why is this trend of oxidative fiber perturbations not explicitly reported in cancer studies? One of the reasons could be in the specifics of our cancer model. As described before, *esg>yki*^{act} tumors induce systemic hyperglycemia, which is characterized by high levels of circulating sugars and inhibition of the IIS pathway (Kwon et al 2015). This condition is highly reminiscent of that conferred by type 2 diabetes (insulin-independent), which is why the response from oxidative muscle fibers in our model and diabetic patients is similar. Notably, hyperglycemia is commonly associated with some tumors, especially originating from the gastrointestinal tract (Tayek, J.A., 1992). There is a scarcity of information of how hyperglycemia may influence oxidative fiber loss, but our study certainly predicts such a link.

One interesting aspect of our results is the atypical deposition of glycogen to the TDTs in cachectic flies. One possible explanation is that, in acute cases, TDTs compensate for the physiological burden of hyperglycemic conditions by accumulating glycogen. Interestingly, higher amounts of type IIx fibers are seen in type 2 diabetes patients (Mogensen et al. 2007). Type IIx fibers have higher glycogen content and glycolytic activity, and it is suggested that they are naturally resistant to the effects of insulin resistance and type 2 diabetes (Lebrasseur et al. 2010). Thus, accumulation of glycogen in TDTs may represent a physiological mechanism for regulating circulating sugar comparable to increasing amounts of type IIx fibers in type 2 diabetes patients. Certainly, these data underscore the differences in carbohydrate control between IFMs and TDTs. Thoroughly analyzing the expression of metabolic genes in *esg>yki*^{act}

TDTs would further elucidate the possible mechanisms by which TDTs and their mammalian counterparts circumvent wasting and metabolic dysregulation.

We were particularly interested in identifying genetic factors that are involved in the different response demonstrated by IFMs and TDTs in the presence of gut tumors. Through comparative gene expression analysis, we identified the evolutionarily conserved transcription factor, *cbt*, as one of the candidates. Notably, *cbt* overexpression in IFMs, but not TDTs, induced functional impairment, mimicking the fiber-specific susceptibility of *esg>yki*^{act} flies to tumor presence. Our findings of extreme IFM glycogen depletion suggest that *cbt* does modulate carbohydrate control. Indeed, ubiquitous knockdown of *cbt* induces sugar intolerance, suggesting a role in carbohydrate metabolism (Havula et al. 2013). Considering its role in sugar tolerance, *cbt* induction in the hyperglycemic *esg>yki*^{act} flies may represent a compensatory response gone too far (i.e. IFM death).

The most surprising similarity between *cbt*-overexpressing (*fln>cbt*) and cachectic (*esg>yki*^{act}) IFMs was the characteristic morphology featuring hollow formations within muscle fibers (which we termed 'perforations'). These features were detected at the time points preceding mass fiber degeneration. We are not positive that the perforations originate from swollen membranous structures, as these perforations stain neither for mitochondria nor t-tubule cisternae markers. Furthermore, nuclei were localized to the peripheries, wholly within the perforations. Based on our combined analysis, we suspect that sarcoplasmic swelling may explain the perforations. One possible explanation for the swelling could be the cells adjusting osmolarity to normal physiological levels in response to an excess of an unknown metabolite in the cytosol. Given the aberrations in carbohydrate metabolism, such an accumulation of metabolites is plausible. Hypo-osmotic swelling poses a significant threat to cell membrane integrity, and as such, may contribute to IFM death (Pietuch et al. 2013). Further investigation, including electron microscopy studies, will be necessary to establish any definitive explanation.

Our finding that *cbt* overexpression in the TDTs induced significant muscle hypertrophy was unexpected yet underscored the contrast between IFMs and TDTs. Unlike mammalian skeletal muscle, fiber number and composition are immutable in adult *Drosophila* somatic muscles (Piccirillo et al. 2014). Thus, our results strongly suggest that *cbt* plays a critical role in TDT myogenesis. One report that stimulation of TGF-β signaling increases TDT fiber number strongly support this notion as well (Jaramillo et al. 2009). Further supporting its developmental role, *cbt* was shown to be a required factor for dorsal closure (Muñoz-Descalzo et al. 2005). Differential gene expression analysis would be instrumental in determining the downstream effectors of this developmental role.

Collectively, our findings emphasize that differing metabolic requirements dramatically influence the susceptibility of fiber types to muscle wasting. Metabolically active muscles, such as IFMs, are more acutely affected than the sporadically active TDTs. We also present strong evidence implicating *cbt* as a critical factor mediating cachectic muscle wasting, but little is known about the gene targets downstream of *cbt*. However, we have identified several genes that may be responsible. Our gene enrichment analysis suggests that genes involved in the biosynthesis of carbohydrate derivatives are differentially regulated, which may explain our hypothesis that an accumulation of metabolites in the cytosol induces hypo-osmotic stress. The upregulation of the oxidoreductase *Cyp4p3* in both *esg>yki*^{act} and *fln>cbt* flies is particularly interesting, as oxidoreductases are suspected drivers of oxidative stress (Kussmaul and Hirst 2006). We also found that *tobi*, an enzyme involved in the breakdown of polysaccharides (like glycogen) was commonly upregulated (Davies and Henrissat 2015). Attenuation of *tobi* expression by RNAi knockdown may protect glycogen reservoirs from depletion.

Thus, our study provides important clues in the search of physical effectors driving cachexia. Furthermore, we have identified a novel role of *cbt* in specifying TDT fiber number in *Drosophila* development.

INTEGRATION OF THESIS RESEARCH

In this work, we have identified potential causes, at the molecular scale, of cachexia-like muscle wasting in *Drosophila*. We anticipate, given the conserved sequence and function of *cbt*, that our findings will hold relevance in studies of muscle wasting in murine and human models.

In pursuit of the molecular mechanisms underlying cachexia, various fields of biology were incorporated. This project was fundamentally rooted in organismal biology, genetics, histochemistry, bioinformatics, and molecular biology. *Drosophila* researchers are outfitted with potent tools, like the GAL4/UAS system, to modulate the expression and function of genes. Without these tools, this study would certainly not have been possible. Moreover, the use of PCR, next-generation sequencing, and bioinformatic techniques was invaluable in our search for genes of interest. Histochemical techniques such as the SDH and PAS assays for mitochondrial activity and glycogen presence were critical to characterize the detrimental effects of *cbt* on flight muscles. Furthermore, our understanding of mammalian skeletal muscle physiology allowed us to draw conclusions that may provide insight into the etiology of fiber-specific muscle wasting.

ACKNOWLEDGEMENTS

I would like to thank the Office of the Vice President for Research for the funding that made this project (and academic opportunity) possible. I would also like to thank the College of Science and Mathematics for funding the Masters of Science in Integrative Biology teaching assistantship. Thank you to the directors of the Histology and Microscopy core facilities for the technical support. I would also like to thank my committee members for their useful insight and withering sarcasm. Of course, thank you to my advisor, Anton Bryantsev, for his tireless efforts to ensure funding, as well as his commitment to my education and personal development. I appreciate the great help from my lab mates, and particularly our post-doc, Maria Chechenova, for her guidance. Special thanks to my fellow graduate students – Kelsey, Kristina, Bradley, everyone. Finally, I want to thank my girlfriend Andrea for her incredible support during this time.

MATERIALS AND METHODS

***Transgenic Flies and Drosophila Stocks*.** Transgenic fly stocks to regulate gene expression are shown in Table 5; In driver lines, the gene *GAL4*, a yeast transcriptional activator, is inserted under control of native regulatory elements enabling its expression in different tissues or developmental times. Within these tissues, GAL4 specifically binds to the enhancers containing the upstream-activated sequence (*UAS*), exported from yeast and strategically placed upstream of genes of interest, for ectopic gene transcription. For targeted gene downregulation, *UAS*-controlled constructs express double-strand RNA molecules matching the sequence of targeted transcripts to eliminate them via the phenomenon of RNA interference. All stock lines were maintained at room temperature. For most crosses, virgin females were collected regularly from the *GAL4* stocks. Crosses were made using *GAL4* females and *UAS* or control males. Transgenic flies were reared in separate incubators kept at 18°C, 25°C, and 29°C, or at room temperature. *esg>yki*^{act} crosses began at 18°C, and virgin adult flies were relocated to 29°C to induce neoplasia. Crosses involving *fln-GAL4* and *Act79B6-GAL4* were maintained at 29°C. All aging of flies was done at 29°C and flies were moved to fresh food twice per week.

Flight and Jump tests. Newly emerging flies were collected and reared at 29°C for 2 days, 1 week, and 2 weeks. At time of testing, flies were allowed to acclimate to room temperature for 30-60 minutes. Individually, flies were released into the testing chamber (lit from above and partioned into regions designated as Up, Horizontal, Down, and Null/Nonflying). The landing location of each fly was then recorded. After tests, flies were knocked out at cold temperature (4°C) and recollected for histological analysis. For jump tests, wings were clipped and flies were allowed a 24-hour recovery period. Flies were then released individually onto a paper sheet

where jump distance could be marked (start and end points, then measured). If necessary, flies were coaxed to jump with light touches from a paintbrush.

Cryosectioning. Flies were snap-frozen in liquid nitrogen and sectioned on a Leica CM1850 cryostat. Section thickness for immunofluorescent analysis was maintained at 7µm, for histochemistry – 14 µm. Serial sections were collected on microscope slides and air-dried.

Immunofluoresecence staining. ¥ Sections (7 µm) were fixed in 3.7% formaledehyde and then rinsed in 1X Phosphate Buffered Solution (PBS). After fixation, sections were permeabilized in a solution of 1X PBS containing 1% Triton X-100. Alexa Fluor 488 phalloidin was used to stain F-actin (1:1000), and DAPI was used for DNA staining. Immunostaining against alpha and beta integrins was done using DK.1A4 and CF.6G11 monoclonal antibodies (1:100), which were obtained from the Developmental Studies Hybridoma Bank (DSHB) (DK.1A4 and CF.6G11 were originally deposited to DSHB by Brower, D.). To stain t-tubules, 4F3 α-Dlg antibody was used (DSHB, 1:100). For mitochondrial staining, Alexa Fluor 568 Streptavidin (S11226) was used, owing to high biotinylated protein moetries present in the mitochondrial matrix and involved in carboxylation of organic acids (Praul et al. 1998).

Succinate Dehydrogenase (SDH) Assay. We adopted the protocol published by Deak in 1977. Fresh sections (14 µm) were incubated in a solution containing sodium succinate (500 mM), Nitro-BT (4 mg/ml), Tris-HCl pH 7.4 (0.2 M), $MgCl_2$ (50 mM), H_2O, and sodium azide (100 mM). After 5 minutes of incubation, sections were rinsed in 1X PBS. Sections were then fixed in 3.7% formaldehyde, rinsed in 1X PBS, and mounted on slides with a coverslip.

Periodic acid-Schiff (PAS) staining. Standard PAS histochemical protocol was used. Sections (14 µm) were fixed in 3.7% formaldehyde and then rinsed in 1X PBS. After fixation, sections were incubated in 0.5% periodic acid for 25 minutes, then rinsed in distilled water.

Following oxidation, sections were incubated in Schiff's reagent for 15 minutes, then rinsed in distilled water for 5 minutes, dried, and mounted.

Microscopy. For fly collection, freezing, and muscle dissections, a Leica MZ75 dissecting microscope was used. For imaging of SDH and PAS assays, a Zeiss Axio Imager M2 was used. Fluorescence micrographs were taken on a Zeiss LSM 700 Confocal microscope.

Muscle Dissections. Muscles were dissected using syringe needles (23G and 27G) under a dissecting miscroscope. Adult flies collected for dissection (all reared at 29°C for 1 week) were moved to TissueTek OCT and then washed three times in 1X PBS solution. Fly thoraces(8 for IFMs and up to 20 for TDTs) were split in 1M sucrose and flight muscles were dissected and relocated into the lysis RLT buffer supplied by the Qiagen RNeasy Mini Kit. Dissected flight muscles were stored at -20°C until ready for RNA purification.

RNA purification. Homogenization of dissected muscle tissue was performed with washed glass beads (0.5mm) in RLT buffer. RNA purification was done using the RNeasy Mini Kit (Qiagen) protocol. Final concentrations were measured with the Thermo Scientific NanoDrop Lite spectrophotometer. Typically, we obtained 100-200 ng of total RNA per sample. Samples for RNA-seq were then stored at -80°C until shipped. Samples for cDNA synthesis were stored at -20°C.

PCR and cDNA synthesis. All PCRs were performed used the LabNet MultiGene OptiMax thermocycler with Clontech Advantage 2 polymerase mix. cDNA synthesis was performed with random DNA hexamers (50 µM), dNTPs (10 mM), 5X FS Buffer, DTT (0.1 M), and Superscript II reverse transcriptase (Invitrogen). After synthesis, samples were diluted 1:5 in 1X TE buffer.

Next-Gen Sequencing. Total mRNA samples obtained from dissected muscles were outsourced to the Columbia Genome Center for RNA-sequencing. Samples were sequenced

using Illumina HiSeq 2500. Sequencing parameters used: 30 million single-end reads averaging 100 bp. Post-run analysis was performed using the Galaxy online bioinformatics platform (usegalaxy.org). Alignment of unique reads to the *D. melanogaster* genome (flybase.org) was performed using RNA Star, and CuffLinks was used to map data to all known transcript isoforms and for normalization of read counts. Results were further normalized to the expression of muscle-specific *Mef2* gene, stably expressed in all muscle types. Gene alignment for secondary analysis to probe commonly and differentially regulated genes was done with transcriptome mapping tool Salmon. Statistical divergence between samples was analyzed with DEseq2.

Statistics. For jump muscle measurements (fiber number, surface area), mean measurements and standard deviations could be calculated. For binary data such as flight tests and incidence rates, two-proportion z-tests were used to evaluate statistical significance (for further information on the method, see http://influentialpoints.com/Training/z-test_for_independent_proportions-principles-properties-assumptions.htm). In z-tests, experimental groups were always compared against age-matched, isogenic controls (e.g. two-day old *esg*>+ would be paired against two-day old *esg>yki*^{act} flies). To calculate z-values, the following formula was used:

$$z = \frac{(p_1 - p_2)}{\sqrt{p(1 - p)\left(\frac{1}{n_1} + \frac{1}{n_2}\right)}}$$

Where:

p_1 and p_2 are the two sample proportions

n_1 and n_2 are the two population sizes

p is the estimated true proportion under the null hypothesis equal to

$$\frac{n_1 p_1 + n_2 p_2}{n_1 + n_2}$$

FIGURES AND TABLES

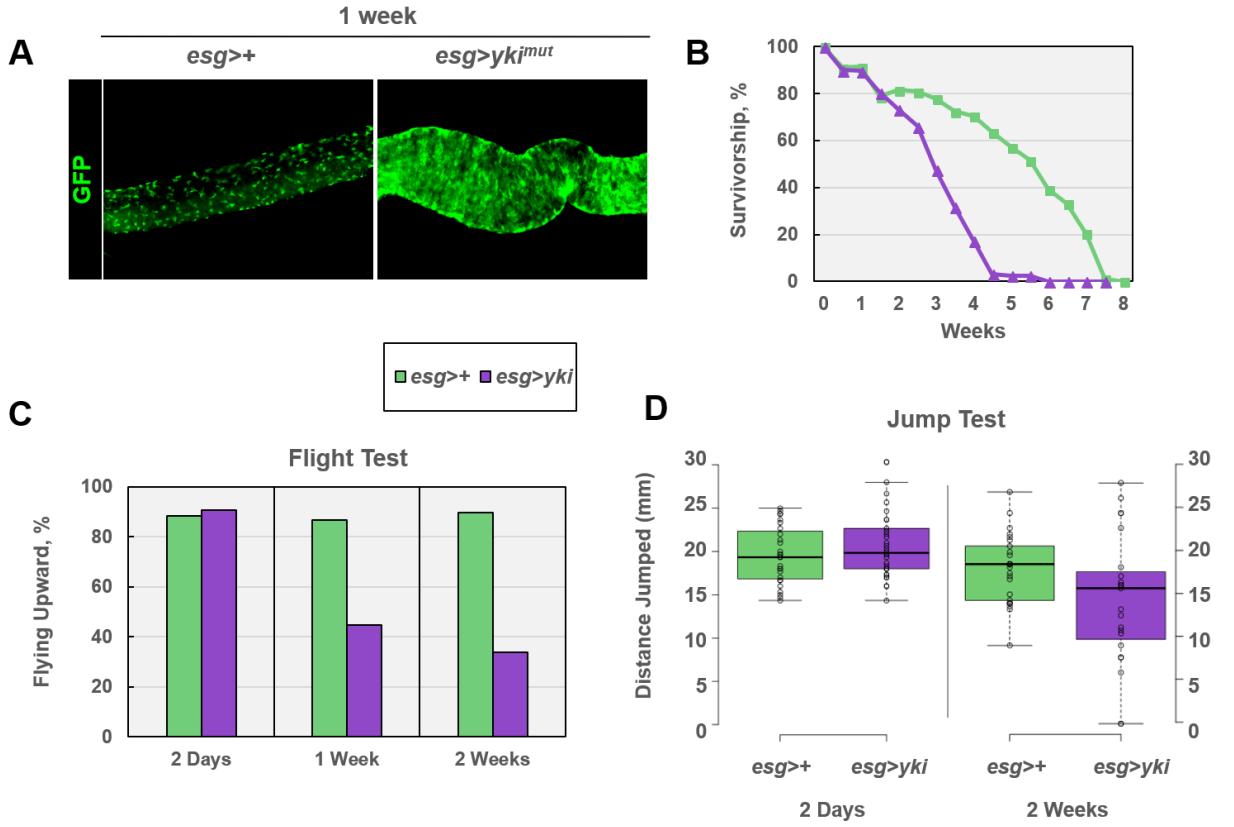

Figure 1: *esg>yki^{act}* flight muscles are more susceptible to loss of function than jump muscles (A) Dissected midguts of control (*esg*>+) and neoplasia producing *esg>yki^{act}*. GFP expression is driven in intestinal stem cells by *esg-GAL4,UAS-GFP*. Note dramatic enrichment of GFP-positive cells in *esg>yki^{act}* midguts. **(B)** Survivorship plot over 8 weeks. Control and *esg>yki^{act}* are represented by green and purple lines, respectively. **(C)** Assay testing functional state of flight muscles, shown as percentage of control (green) and *esg>yki^{act}* (purple) flies able to fly upwards. See Table 1 for statistical analysis. **(D)** Assay testing functional state of jump muscles, jumping distance (mm) of control (green) and *esg>yki^{act}* (purple) flies shown with box plot.

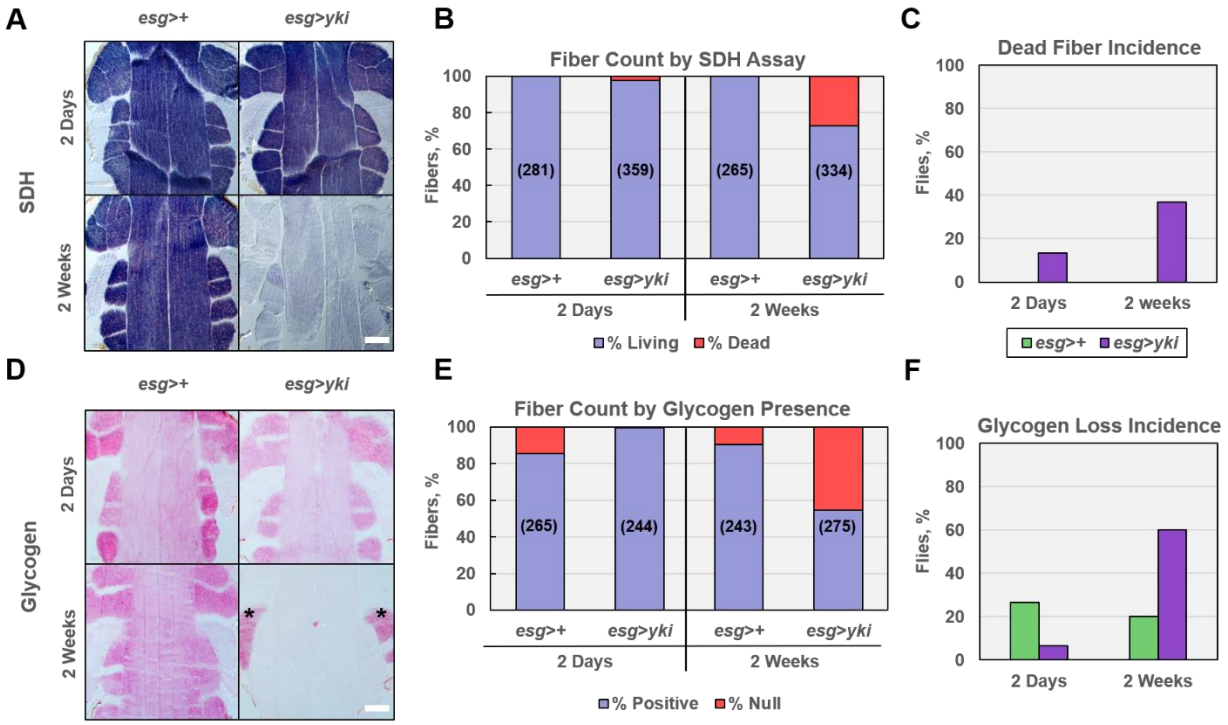

Figure 2: Mitochondrial damage and glycogen loss in *esg>yki^{act}* flight muscles (A) Sectioned thoraces stained by histochemistry to show succinate dehydrogenase (SDH) activity; Note that IFMs are strongly positive for SDH (dark purple/blue staining); scale = 100µm **(B)** Quantification of SDH positive (living) and SDH negative (dead) flight muscle fibers. Total fibers assessed in parentheses. **(C)** Incidence of flies with at least one SDH-negative flight muscle fiber. 15-20 flies were assessed per group. See Table 2 for statistical analysis. **(D)** Sectioned thoraces stained for glycogen content with periodic acid Schiff (PAS) assay; IFMs, not TDTs, are normally positive for glycogen (pink staining), however glycogen-positive jump muscles can be seen in *esg>yki^{act}* flies (indicated by asterisk, *); scale = 100µm **(E)** Quantification of flight muscle fibers positive and negative for glycogen in PAS assay. Total fibers assessed in parentheses. **(F)** Incidence of flies with at least one flight muscle fiber lacking glycogen. 15 flies were assessed per group. See Table 2 for statistical analysis.

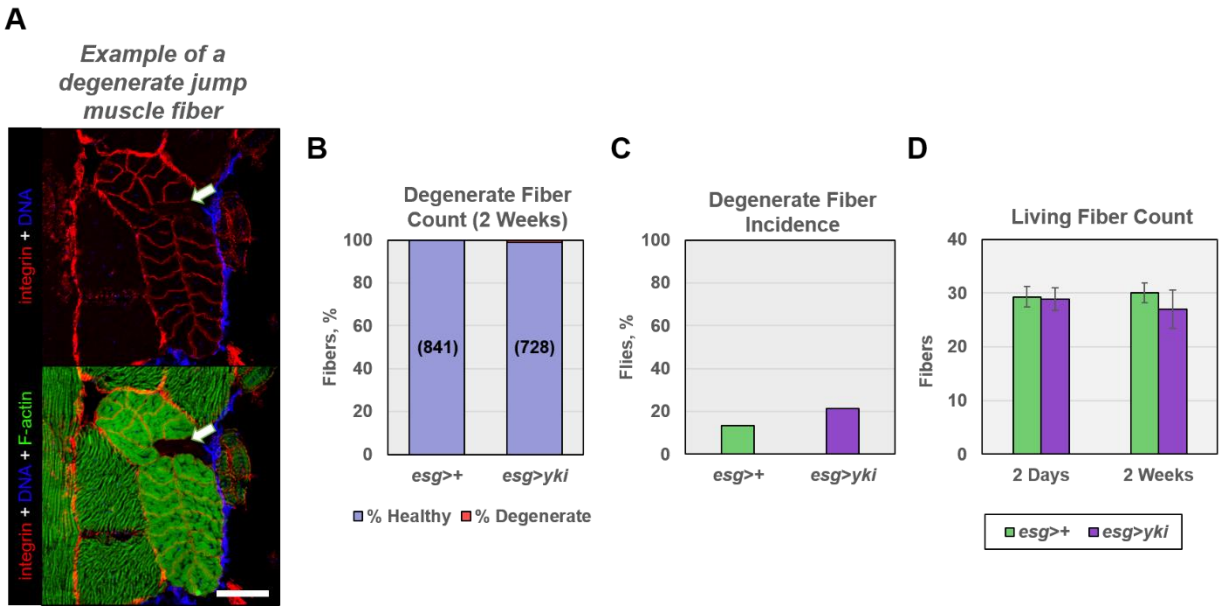

Figure 3: *esg>yki^{act}* jump muscles do not degenerate (A) Example of a degenerate jump muscle fiber (arrows), which can be detected by the lack of F-actin positive staining (green) and nuclei (blue) Individual fibers within the TDT are revealed by immunostaining of the transmembrane surface integrins (red); scale = 50µm **(B)** Quantification of degenerate jump muscle fiber counts by presence/absence of F-actin. Control (green) and *esg>yki^{act}* (purple). Number of fibers assessed are in parentheses. **(C)** Incidence of degenerate jump muscle fibers in two-week old flies. **(D)** Quantification of living jump muscle fiber counts. Measurements shown are mean ± SDs.

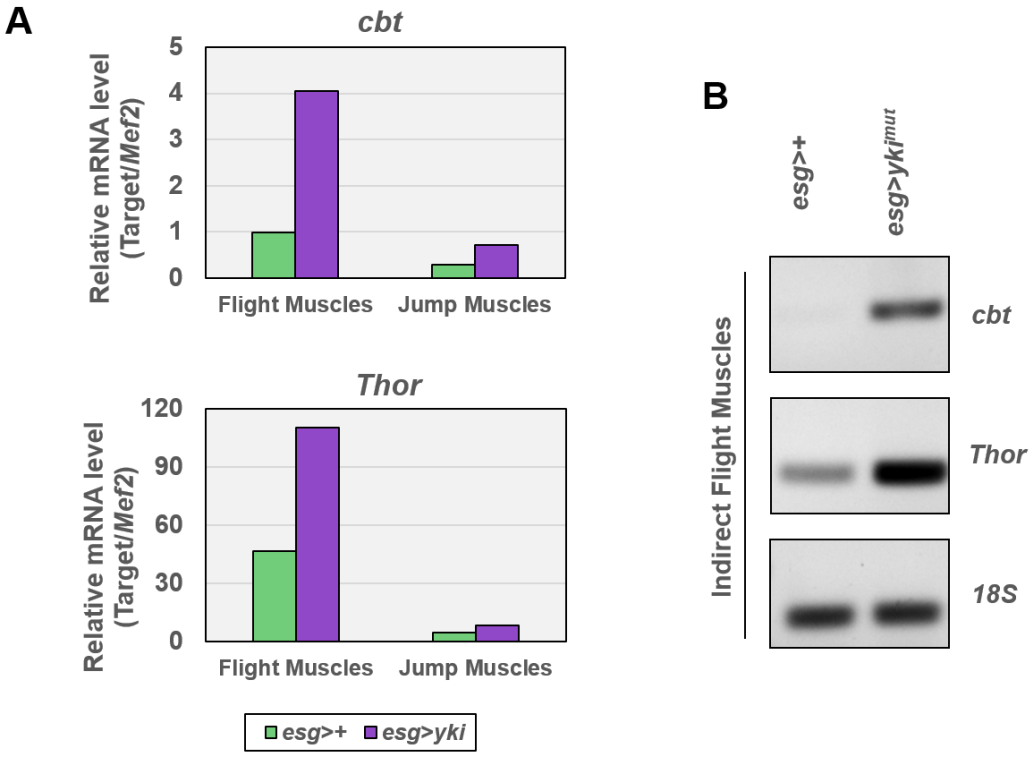

Figure 4: Identification of two candidate genes, *cbt* and *Thor* **(A)** Relative mRNA expression (normalized to *Mef2* levels) of candidate genes from dissected flight muscles (top graph) from dissected jump muscles (bottom graph), as revealed by next-gen sequencing. **(B)** Confirmation of *cbt* and *Thor* overexpression by endpoint PCR of cDNA synthesized from extracted flight muscles. Top represents genotype; Right represents amplification target. Amplification of 18S rRNA was used as loading control.

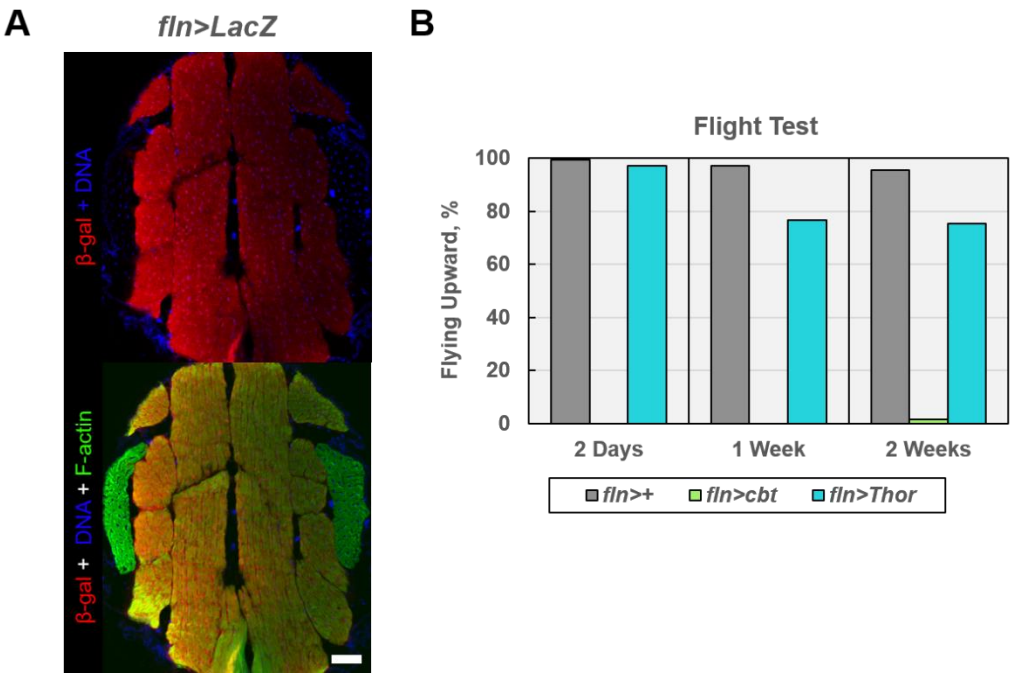

Figure 5: *cbt* overexpression eliminates flight muscle functionality (A) Flight muscle specific expression pattern of the *fln* driver, as shown by β-galactosidase expression from LacZ transgene (red); F-actin and nuclei are counterstained by green and blue, respectively; scale = 50µm **(B)** Percentage of control (gray; *fln*>+), *cbt*-overexpressing (green; *fln>cbt*) and *Thor*-overexpressing (blue; *fln>Thor*) flies able to fly upward. See Table 1 for statistical analysis.

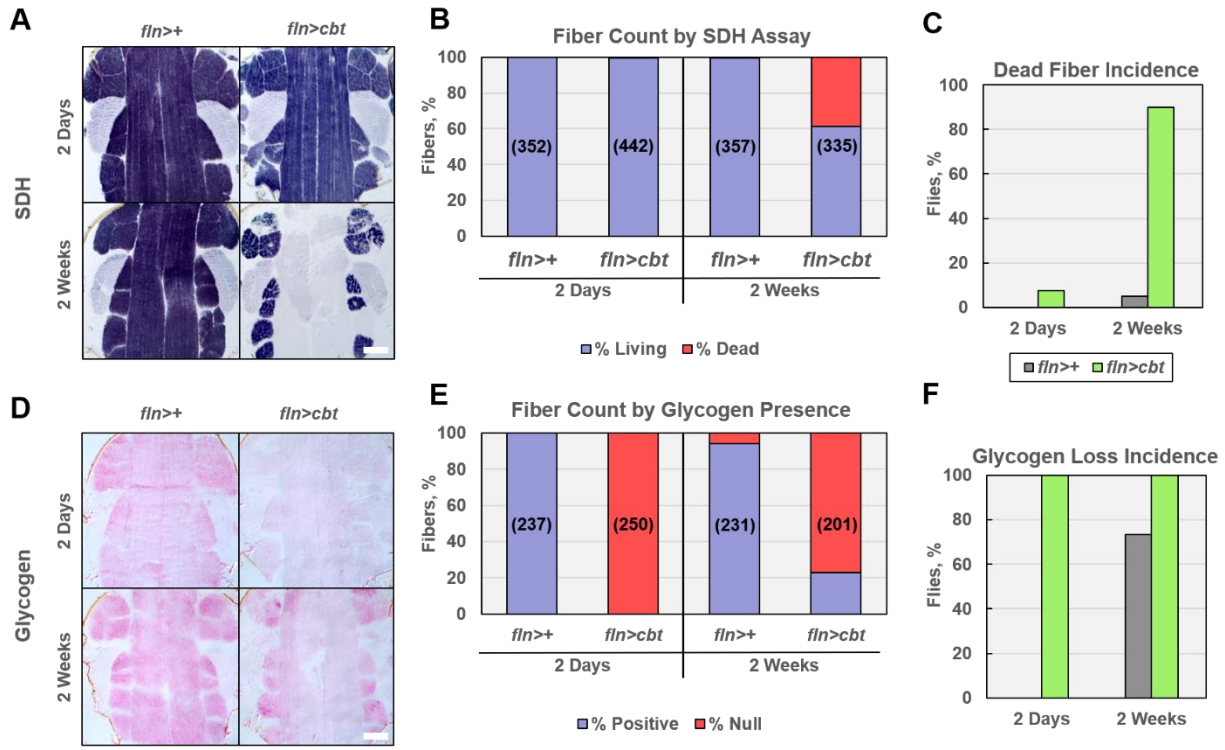

Figure 6: Extensive mitochondrial damage and glycogen deficiency in fln>cbt flight muscles **(A)** Sectioned thoraces stained by histochemistry to show succinate dehydrogenase (SDH) activity; scale = 100µm **(B)** Quantification of SDH positive (living) and SDH negative (dead) flight muscle fibers. Total fibers assessed in parentheses. **(C)** Incidence of flies with at least one SDH-negative flight muscle fiber. 19-26 flies were assessed per group. See Table 2 for statistical analysis. **(D)** Periodic Acid Schiff assay (glycogen stain) images; scale = 100µm **(E)** Quantification of flight muscle fibers positive and negative for glycogen in PAS assay. Total fibers assessed in parentheses. **(F)** Incidence of flies with at least one flight muscle fiber lacking glycogen. 15 flies were assessed per group. See Table 2 for statistical analysis.

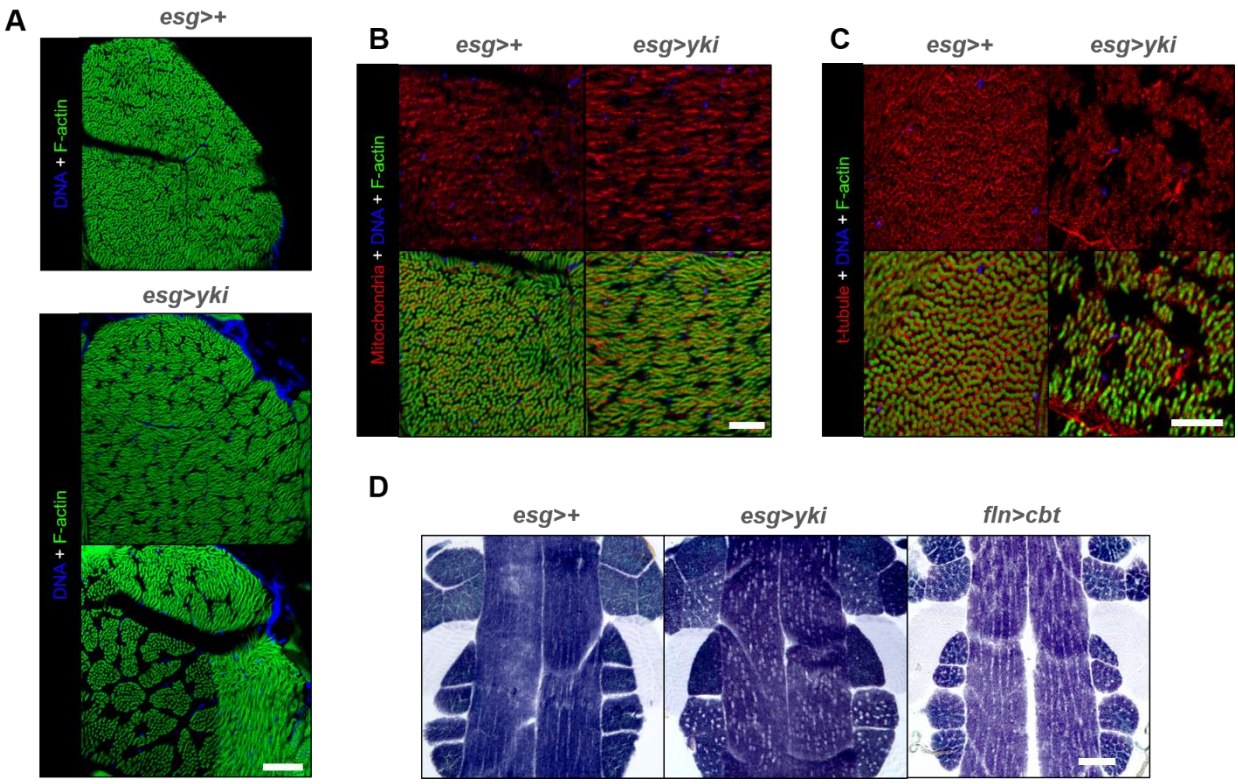

Figure 7: Characterization of perforations in flight muscles of *esg>yki^{act}* and *fln>cbt* flies. **(A)** Magnified view of a transverse section of dorsal-ventral flight muscles showing varying severity of morphological changes of *esg>yki^{act}* flies. *yki^{act}* transgene was induced for 7 days; scale = 50µm **(B)** Staining for mitochondrial biotin with streptavidin (red) to reveal mitochondria in flight muscles; scale = 20µm **(C)** t-tubule immunofluorescence staining with anti-Dlg antibody (red); scale = 10µm **(D)** SDH assay images showing morphological similarities in the flight muscles of *esg>yki^{act}* and *fln>cbt* flies; scale = 100µm

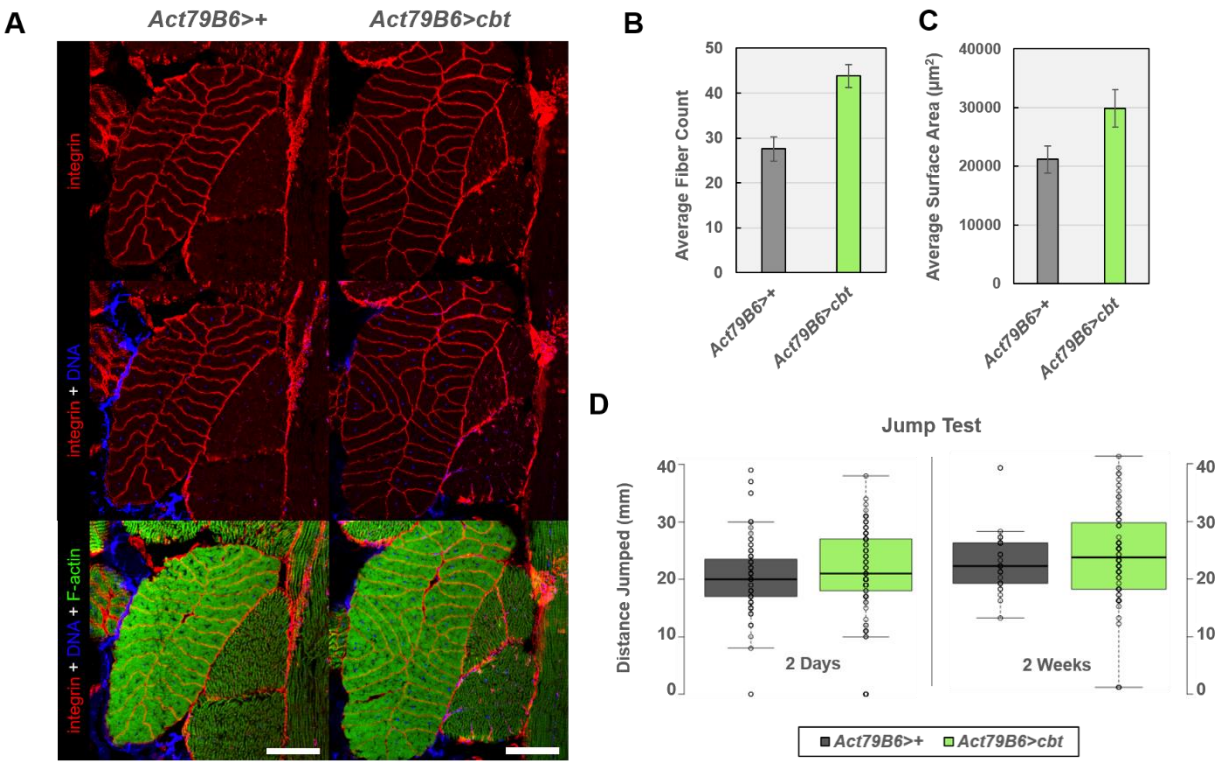

Figure 8: *cbt* overexpression within jump muscles induces hypertrophy while sparing jumping ability (A) Morphology of control (*Act79B6>+*) and *Act79B6>cbt* jump muscles. Individual fibers within the TDT revealed by immunofluorescence staining with α and β-integrin antibodies (red) and costained for F-actin (green) and nuclei (blue); scale = 50µm **(B)** Quantification of living jump muscle fiber counts. Values shown are means ± SDs. **(C)** Quantification of jump muscle surface area (µm^2). Values shown are means ± SDs. **(D)** Quantification of jumping distance (mm).

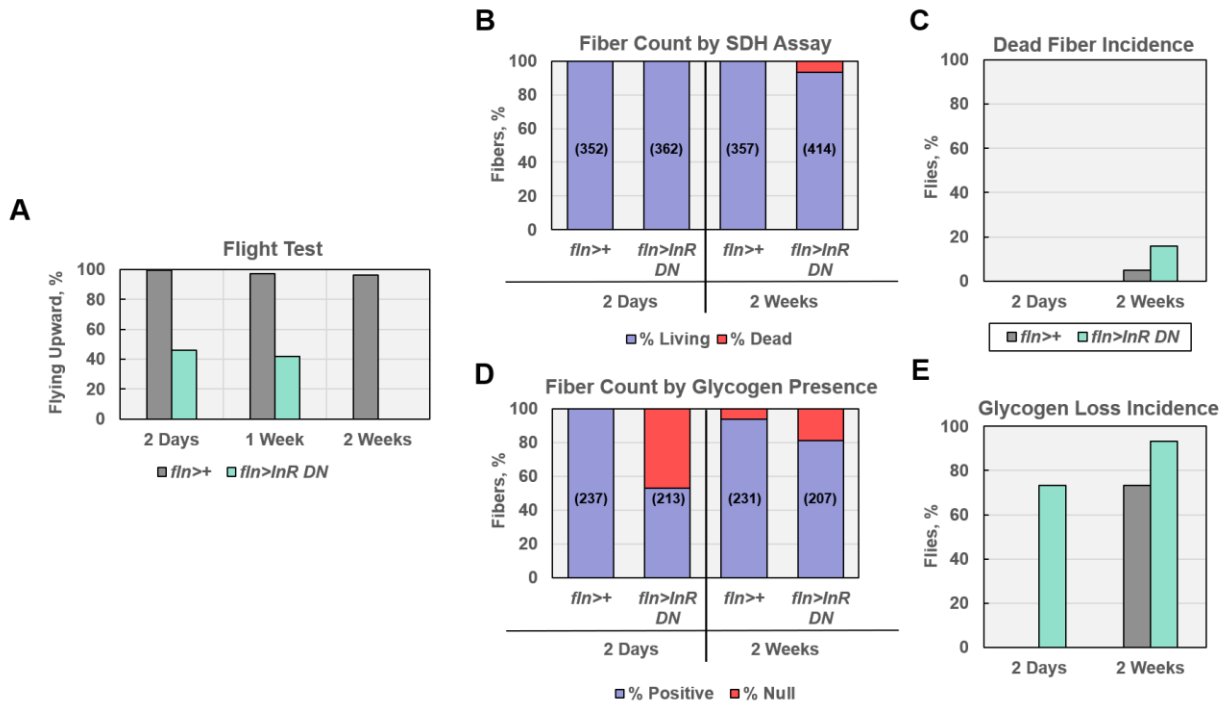

Figure 9: Suppression of insulin signaling impairs flight muscle function, glycogen storage, and mitochondrial activity (A) Percentage of control flies (*fln*>+) and experimental flies overexpressing a dominant-negative insulin receptor (*fln*>*InR*^{DN}) able to fly upward. See Table 1 for statistical analysis. **(B)** Quantification of SDH positive (living) and SDH negative (dead) flight muscle fibers. Total fibers assessed in parentheses. **(C)** Incidence of flies with at least one SDH-negative flight muscle fiber. 20 flies were assessed per group. See Table 2 for statistical analysis. **(D)** Quantification of flight muscle fibers positive and negative for glycogen in PAS assay. Total fibers assessed in parentheses. **(E)** Incidence of flies with at least one flight muscle fiber lacking glycogen. 15 flies were assessed per group. See Table 2 for statistical analysis.

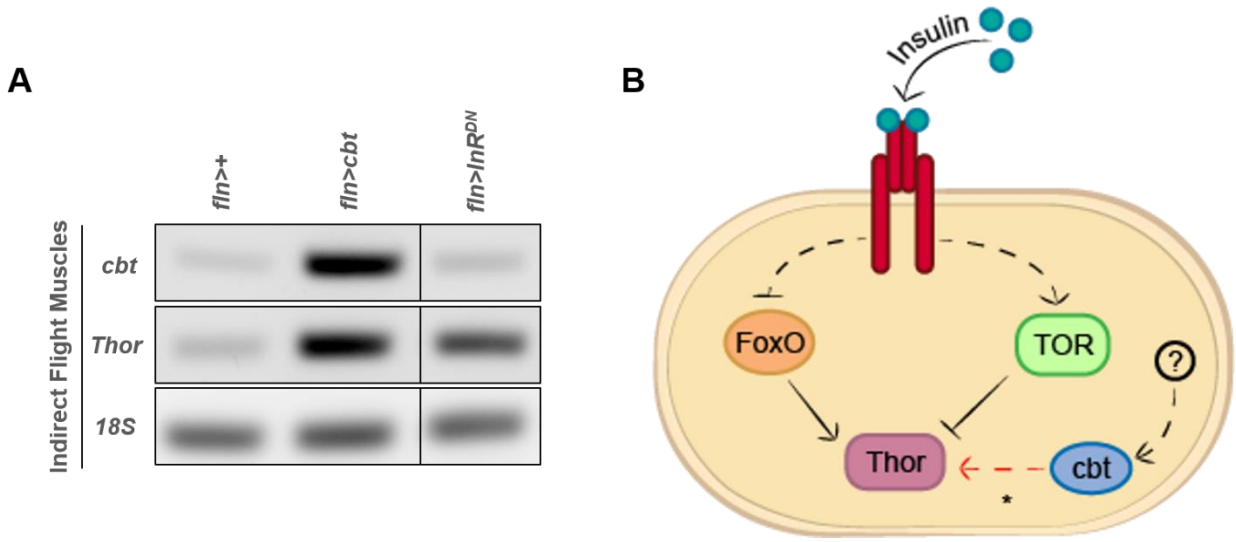

Figure 10: *cbt* is not under regulation by the insulin/insulin-like signaling pathway
(A) Gene expression of *cbt* and *Thor* shown by endpoint PCRs of cDNA synthesized from extracted flight muscles. Top represents genotype, Left represents amplification target. Amplification of 18S rRNA was used as loading control. **(B)** Proposed place for *cbt* in the cell signaling network. Novel finding is indicated by asterisk (*), unknown nature of genetic interaction indicated by red arrow.

Table 1. Two-proportion Z-test analysis performed on all flight test results, comparing experimental groups with respective, age-matched controls. See Materials and Methods.

Two-Proportion Z-Tests					
Flight Tests					
Genotype	Age	N, Experimental	Standard Error	z-value	p-value
esg>yki^{act}	2 Days	51	0.039	1.995	p<0.05
esg>yki^{act}	1 Week	47	0.093	6.192	p<0.01
esg>yki^{act}	2 Weeks	49	0.094	8.195	p<0.01
fln>cbt	2 Days	65	0.067	14.781	p<0.01
fln>cbt	1 Week	62	0.071	13.577	p<0.01
fln>cbt	2 Weeks	65	0.078	12.072	p<0.01
fln>Thor	2 Days	65	0.017	1.482	0.1404
fln>Thor	1 Week	34	0.049	4.21	p<0.01
fln>Thor	2 Weeks	81	0.051	3.955	p<0.01
fln>InR^{DN}	2 Days	65	0.054	9.821	p<0.01
fln>InR^{DN}	1 Week	72	0.06	9.317	p<0.01
fln>InR^{DN}	2 Weeks	71	0.076	12.628	p<0.01

Table 2. Two-proportion Z-test analysis performed on all fiber count incidences (SDH and glycogen counts), comparing experimental groups with respective, age-matched controls.

Two-Proportion Z-Tests					
Incidences of SDH-negative Fibers					
Genotype	Age	N, Experimental	Standard Error	z-value	p-value
esg>yki^{act}	2 Days	20	0.091	-1.469	0.16384
esg>yki^{act}	2 Weeks	19	0.14	-2.636	p<0.05
fln>cbt	2 Days	26	0.059	-1.3	0.20852
fln>cbt	2 Weeks	20	0.158	-5.383	p<0.01
fln>InR^{DN}	2 Days	20	-	-	-
fln>InR^{DN}	2 Weeks	25	0.094	-1.167	0.25776
Incidences of Glycogen-deficient Fibers					
Genotype	Age	N, Experimental	Standard Error	z-value	p-value
esg>yki^{act}	2 Days	15	0.136	1.469	0.16407
esg>yki^{act}	2 Weeks	15	0.179	-2.236	p<0.05
fln>cbt	2 Days	15	0.183	-5.477	p<0.01
fln>cbt	2 Weeks	15	0.124	-2.15	p<0.05
fln>InR^{DN}	2 Days	15	0.176	-4.166	p<0.01
fln>InR^{DN}	2 Weeks	15	0.136	-1.469	0.16407

Table 3. Biological functions overrepresented among genes altered in IFMs by midgut tumors (*esg>yki*^{act}) and *cbt* overexpression.

Downregulated genes (>2-fold)					
GO term	Biological Process	Genes Found	Genes Expected	Fold Enrichment	p-value
GO:0015991	ATP hydrolysis coupled proton transport	4	0.15	25.86	2.66E-02
GO:0002181	cytoplasmic translation	8	0.47	16.94	3.33E-08
Upregulated genes (>2-fold)					
GO term	Biological Process	Genes Found	Genes Expected	Fold Enrichment	p-value
GO:0015986	ATP synthesis coupled proton transport	5	0.04	>100	1.19E-09
GO:0006120	mitochondrial electron transport, NADH to ubiquinone	4	0.06	61.97	6.86E-07
GO:0042775	mitochondrial ATP synthesis coupled electron transport	6	0.14	42.46	6.53E-09
GO:1901137	carbohydrate derivative biosynthetic process	6	0.47	12.83	5.82E-06
GO:0007005	mitochondrion organization	4	0.35	11.35	4.08E-04

Table 4. Candidate genes for further analysis, selected from transcriptome data based on their molecular and biological functions.

Gene	Molecular Function	Biological Function	Expression in yki and cbt
Cyp4p3	Oxidoreductase	Oxidation-reduction	Upregulated
TotA	Unknown	Oxidative stress response	Downregulated
tobi	O-glycosyl hydrolase	Carbohydrate metabolism	Upregulated

Table 5. List of transgenic lines and their genotypes used in this study with the source and ID number of the lines, if applicable.

ID	Source	Line	Genotype
3605		*w^{1118}*	*w[1118]*
	Courtesy of Young Kwon, Perrimon Lab (Kwon et al. 2015)	*esg^{TS}-GAL4*	*w[*]; P{w[+mW.hs]=GawB}NP5130 P{w[+*]=UAS-GFP.U}2; P{w[+mC]=tubP-GAL80[ts]}2*[¥]
		fln-Gal4	*w[1118], P{w[+mC]=UAS-Gal4}attPZH-51C*
		Act79B6-GAL4	*w[1118], P{w[+mC]=UAS-Gal4}6*
	Courtesy of Young Kwon (Kwon et al. 2015)	*UAS-yki^{act}*	*w[*]; P{w[+mC]=UAS-yki.S111A.S168A.S250A}*[¥]
43373	BDSC	*UAS-cbt*	*w[*]; P{w[+mGS]=GSV1}cbt[C480] ush[C480]*
24854	BDSC	*UAS-$Thor^{act}$*	*w[*]; P{w[+mC]=UAS-Thor.LL}s/TM6C, cu[1] Sb[1]*
8252	BDSC	*UAS-InR^{K1409A}*	*y[1] w[1118]; P{w[+mC]=UAS-InR.K1409A}2*

[*], [¥] Presumably

REFERENCES

Acharyya, S., Butchbach, M. E., Sahenk, Z., Wang, H., Saji, M., Carathers, M., ... & Muscarella, P. (2005). Dystrophin glycoprotein complex dysfunction: a regulatory link between muscular dystrophy and cancer cachexia. *Cancer cell*, *8*(5), 421-432.

Aoyagi, T., Terracina, K. P., Raza, A., Matsubara, H., & Takabe, K. (2015). Cancer cachexia, mechanism and treatment. *World journal of gastrointestinal oncology*, *7*(4), 17.

Argilés, J. M., Busquets, S., Stemmler, B., & López-Soriano, F. J. (2014). Cancer cachexia: understanding the molecular basis. *Nature reviews Cancer*, *14*(11), 754.

Bartok, O., Teesalu, M., Ashwall-Fluss, R., Pandey, V., Hanan, M., Rovenko, B. M., ... & Nahmias, Y. (2015). The transcription factor Cabut coordinates energy metabolism and the circadian clock in response to sugar sensing. *The EMBO journal*, *34*(11), 1538-1553.

Barton-Davis, E. R., Shoturma, D. I., Musaro, A., Rosenthal, N., & Sweeney, H. L. (1998). Viral mediated expression of insulin-like growth factor I blocks the aging-related loss of skeletal muscle function. *Proceedings of the national academy of sciences*, *95*(26), 15603-15607.

Bodine, S. C., Latres, E., Baumhueter, S., Lai, V. K. M., Nunez, L., Clarke, B. A., ... & Pan, Z. Q. (2001). Identification of ubiquitin ligases required for skeletal muscle atrophy. *Science*, *294*(5547), 1704-1708.

Bodine, S. C., Stitt, T. N., Gonzalez, M., Kline, W. O., Stover, G. L., Bauerlein, R., ... & Yancopoulos, G. D. (2001). Akt/mTOR pathway is a crucial regulator of skeletal muscle hypertrophy and can prevent muscle atrophy in vivo. *Nature cell biology*, *3*(11), 1014.

Bonaldo, P., & Sandri, M. (2013). Cellular and molecular mechanisms of muscle atrophy. *Disease models & mechanisms*, *6*(1), 25-39.

Borisov, Andrei B., Eduard I. Dedkov, and Bruce M. Carlson. "Interrelations of myogenic response, progressive atrophy of muscle fibers, and cell death in denervated skeletal muscle." *The Anatomical Record* 264.2 (2001): 203-218.

Bottinelli, R. Y. C. R., & Reggiani, C. (2000). Human skeletal muscle fibres: molecular and functional diversity. *Progress in biophysics and molecular biology*, *73*(2-4), 195-262.

Bouché, C., Serdy, S., Kahn, C. R., & Goldfine, A. B. (2004). The cellular fate of glucose and its relevance in type 2 diabetes. *Endocrine reviews*, *25*(5), 807-830.

Boucher, J., Kleinridders, A., & Kahn, C. R. (2014). Insulin receptor signaling in normal and insulin-resistant states. *Cold Spring Harbor perspectives in biology*, *6*(1), a009191.

Bour, B. A., O'Brien, M. A., Lockwood, W. L., Goldstein, E. S., Bodmer, R., Taghert, P. H., ... & Nguyen, H. T. (1995). Drosophila MEF2, a transcription factor that is essential for myogenesis. *Genes & development*, *9*(6), 730-741.

Brand, A. H., & Perrimon, N. (1993). Targeted gene expression as a means of altering cell fates and generating dominant phenotypes. *development*, *118*(2), 401-415.

Bryantsev, A. L., Baker, P. W., Lovato, T. L., Jaramillo, M. S., & Cripps, R. M. (2012). Differential requirements for Myocyte Enhancer Factor-2 during adult myogenesis in Drosophila. *Developmental biology*, *361*(2), 191-207.

Bryantsev, A. L., Duong, S., Brunetti, T. M., Chechenova, M. B., Lovato, T. L., Nelson, C., ... & Cripps, R. M. (2012). Extradenticle and homothorax control adult muscle fiber identity in Drosophila. *Developmental cell*, *23*(3), 664-673.

Bülow, M. H., Aebersold, R., Pankratz, M. J., & Jünger, M. A. (2010). The Drosophila FoxA ortholog Fork head regulates growth and gene expression downstream of Target of rapamycin. *PLoS One*, *5*(12), e15171.

Chevalier, S., & Farsijani, S. (2013). Cancer cachexia and diabetes: similarities in metabolic alterations and possible treatment. *Applied Physiology, Nutrition, and Metabolism*, *39*(6), 643-653.

Ciciliot, S., Rossi, A. C., Dyar, K. A., Blaauw, B., & Schiaffino, S. (2013). Muscle type and fiber type specificity in muscle wasting. *The international journal of biochemistry & cell biology*, *45*(10), 2191-2199.

Coyle, E. F., Sidossis, L. S., Horowitz, J. F., & Beltz, J. D. (1992). Cycling efficiency is related to the percentage of type I muscle fibers. *Medicine and science in sports and exercise*, *24*(7), 782-788.

Davies, G., & Henrissat, B. (1995). Structures and mechanisms of glycosyl hydrolases. *Structure*, *3*(9), 853-859

Deak, I. I. (1977). A histochemical study of the muscles of Drosophila melanogaster. *Journal of morphology*, *153*(2), 307-316.

Demontis, F., & Perrimon, N. (2010). FOXO/4E-BP signaling in Drosophila muscles regulates organism-wide proteostasis during aging. *Cell*, *143*(5), 813-825.

dos Santos, M. P., Batistela, E., Pereira, M. P., Paula-Gomes, S., Zanon, N. M., do Carmo Kettelhut, I., ... & Kawashita, N. H. (2016). Higher insulin sensitivity in EDL muscle of rats fed a low-protein, high-carbohydrate diet inhibits the caspase-3 and ubiquitin-proteasome proteolytic systems but does not increase protein synthesis. *The Journal of nutritional biochemistry*, *34*, 89-98.

Ekengren, S., Tryselius, Y., Dushay, M. S., Liu, G., Steiner, H., & Hultmark, D. (2001). A humoral stress response in Drosophila. *Current biology*, *11*(9), 714-718.

Figueroa-Clarevega, A., & Bilder, D. (2015). Malignant Drosophila tumors interrupt insulin signaling to induce cachexia-like wasting. *Developmental cell*, *33*(1), 47-55.

Fox, K. M., Brooks, J. M., Gandra, S. R., Markus, R., & Chiou, C. F. (2009). Estimation of cachexia among cancer patients based on four definitions. *Journal of oncology*, *2009*.

Fukawa, T., Yan-Jiang, B. C., Min-Wen, J. C., Jun-Hao, E. T., Huang, D., Qian, C. N., ... & Lim, W. J. (2016). Excessive fatty acid oxidation induces muscle atrophy in cancer cachexia. *Nature medicine*, *22*(6), 666.

Fyrberg, E. A., Mahaffey, J. W., Bond, B. J., & Davidson, N. (1983). Transcripts of the six Drosophila actin genes accumulate in a stage-and tissue-specific manner. *Cell*, *33*(1), 115-123.

Gingras, A. C., Kennedy, S. G., O'Leary, M. A., Sonenberg, N., & Hay, N. (1998). 4E-BP1, a repressor of mRNA translation, is phosphorylated and inactivated by the Akt (PKB) signaling pathway. *Genes & development*, *12*(4), 502-513.

Gingras, A. C., Raught, B., & Sonenberg, N. (1999). eIF4 initiation factors: effectors of mRNA recruitment to ribosomes and regulators of translation. *Annual review of biochemistry*, *68*(1), 913-963.

Gingras, A. C., Raught, B., Gygi, S. P., Niedzwiecka, A., Miron, M., Burley, S. K., ... & Sonenberg, N. (2001). Hierarchical phosphorylation of the translation inhibitor 4E-BP1. *Genes & development*, *15*(21), 2852-2864.

Goldspink, G. (1999). Changes in muscle mass and phenotype and the expression of autocrine and systemic growth factors by muscle in response to stretch and overload. *The Journal of Anatomy*, *194*(3), 323-334.

Guillaumond, F., Gréchez-Cassiau, A., Subramaniam, M., Brangolo, S., Peteri-Brünback, B., Staels, B., ... & Teboul, M. (2010). Krüppel-like factor KLF10 is a link between the circadian clock and metabolism in liver. *Molecular and cellular biology*, *30*(12), 3059-3070.

Han, Z., Yi, P., Li, X., & Olson, E. N. (2006). Hand, an evolutionarily conserved bHLH transcription factor required for Drosophila cardiogenesis and hematopoiesis. *Development*, *133*(6), 1175-1182.

Hara, K., Yonezawa, K., Weng, Q. P., Kozlowski, M. T., Belham, C., & Avruch, J. (1998). Amino acid sufficiency and mTOR regulate p70 S6 kinase and eIF-4E BP1 through a common effector mechanism. *Journal of Biological Chemistry*, *273*(23), 14484-14494.

Havula, E., Teesalu, M., Hyötyläinen, T., Seppälä, H., Hasygar, K., Auvinen, P., ... & Hietakangas, V. (2013). Mondo/ChREBP-Mlx-regulated transcriptional network is essential for dietary sugar tolerance in Drosophila. *PLoS genetics*, *9*(4), e1003438.

Hederstedt, L., & Rutberg, L. (1981). Succinate dehydrogenase--a comparative review. *Microbiological reviews*, *45*(4), 542.

Hikida, R. S., Gollnick, P. D., Dudley, G. A., Convertino, V. A., & Buchanan, P. (1989). Structural and metabolic characteristics of human skeletal muscle following 30 days of simulated microgravity. *Aviation, Space, and Environmental Medicine*, *60*(7), 664-670.

Iizuka, K., Takeda, J., & Horikawa, Y. (2011). Krüppel-like factor-10 is directly regulated by carbohydrate response element-binding protein in rat primary hepatocytes. *Biochemical and biophysical research communications*, *412*(4), 638-643.

Jacquemin, V., Furling, D., Bigot, A., Butler-Browne, G. S., & Mouly, V. (2004). IGF-1 induces human myotube hypertrophy by increasing cell recruitment. *Experimental cell research*, *299*(1), 148-158.

Jaramillo, M. S., Lovato, C. V., Baca, E. M., & Cripps, R. M. (2009). Crossveinless and the TGFβ pathway regulate fiber number in the Drosophila adult jump muscle. *Development*, *136*(7), 1105-1113.

Kamei, Y., Miura, S., Suzuki, M., Kai, Y., Mizukami, J., Taniguchi, T., ... & Nishino, I. (2004). Skeletal muscle FOXO1 (FKHR) transgenic mice have less skeletal muscle mass, down-regulated Type I (slow twitch/red muscle) fiber genes, and impaired glycemic control. *Journal of Biological Chemistry*, *279*(39), 41114-41123.

Kir, S., Komaba, H., Garcia, A. P., Economopoulos, K. P., Liu, W., Lanske, B., ... & Spiegelman, B. M. (2016). PTH/PTHrP receptor mediates cachexia in models of kidney failure and cancer. *Cell metabolism*, *23*(2), 315-323.

Kussmaul, L., & Hirst, J. (2006). The mechanism of superoxide production by NADH: ubiquinone oxidoreductase (complex I) from bovine heart mitochondria. *Proceedings of the National Academy of Sciences*, *103*(20), 7607-7612.

Kwon, Y., Song, W., Droujinine, I. A., Hu, Y., Asara, J. M., & Perrimon, N. (2015). Systemic organ wasting induced by localized expression of the secreted insulin/IGF antagonist ImpL2. *Developmental cell*, *33*(1), 36-46.

Langstein, H. N., & Norton, J. A. (1991). Mechanisms of cancer cachexia. *Hematology/oncology clinics of North America*, *5*(1), 103-123.

LeBrasseur, N. K., Walsh, K., & Arany, Z. (2010). Metabolic benefits of resistance training and fast glycolytic skeletal muscle. *American Journal of Physiology-Endocrinology and Metabolism*, *300*(1), E3-E10.

Lindsay, T., Sustar, A., & Dickinson, M. (2017). The function and organization of the motor system controlling flight maneuvers in flies. *Current Biology*, *27*(3), 345-358.

Lowell, B. B., & Shulman, G. I. (2005). Mitochondrial dysfunction and type 2 diabetes. *Science*, *307*(5708), 384-387.

Lundholm, K., Holm, G., & Scherstén, T. (1978). Insulin resistance in patients with cancer. *Cancer research*, *38*(12), 4665-4670.

Mattila, J., & Hietakangas, V. (2017). Regulation of Carbohydrate Energy Metabolism in Drosophila melanogaster. *Genetics*, *207*(4), 1231-1253.

Mavalli, M. D., DiGirolamo, D. J., Fan, Y., Riddle, R. C., Campbell, K. S., van Groen, T., ... & Clemens, T. L. (2010). Distinct growth hormone receptor signaling modes regulate skeletal muscle development and insulin sensitivity in mice. *The Journal of clinical investigation*, *120*(11), 4007-4020.

Meek, S. E., Persson, M., Ford, G. C., & Nair, K. S. (1998). Differential regulation of amino acid exchange and protein dynamics across splanchnic and skeletal muscle beds by insulin in healthy human subjects. *Diabetes*, *47*(12), 1824-1835.

Mendell, J. R., & Engel, W. K. (1971). The fine structure of type II muscle fiber atrophy. *Neurology*, *21*(4), 358-358.

Mogensen, M., Sahlin, K., Fernström, M., Glintborg, D., Vind, B. F., Beck-Nielsen, H., & Højlund, K. (2007). Mitochondrial respiration is decreased in skeletal muscle of patients with type 2 diabetes. *Diabetes*, *56*(6), 1592-1599.

Morimoto, D., Walinda, E., Fukada, H., Sou, Y. S., Kageyama, S., Hoshino, M., ... & Ariyoshi, M. (2015). The unexpected role of polyubiquitin chains in the formation of fibrillar aggregates. *Nature communications*, *6*, 6116.

Muñoz-Descalzo, S., Belacortu, Y., & Paricio, N. (2007). Identification and analysis of cabut orthologs in invertebrates and vertebrates. *Development genes and evolution*, *217*(4), 289-298.

Muñoz-Descalzo, S., Terol, J., & Paricio, N. (2005). Cabut, a C2H2 zinc finger transcription factor, is required during Drosophila dorsal closure downstream of JNK signaling. *Developmental biology*, *287*(1), 168-179.

Murillo-Maldonado, J. M., Sánchez-Chávez, G., Salgado, L. M., Salceda, R., & Riesgo-Escovar, J. R. (2011). Drosophila insulin pathway mutants affect visual physiology and brain function besides growth, lipid, and carbohydrate metabolism. *Diabetes*, 60(5), 1632-1636.

O'Neill, E. D., Wilding, J. P., Kahn, C. R., Van Remmen, H., McArdle, A., Jackson, M. J., & Close, G. L. (2010). Absence of insulin signalling in skeletal muscle is associated with reduced muscle mass and function: evidence for decreased protein synthesis and not increased degradation. *Age*, *32*(2), 209-222.

Oas, S. T., Bryantsev, A. L., & Cripps, R. M. (2014). Arrest is a regulator of fiber-specific alternative splicing in the indirect flight muscles of Drosophila. *J Cell Biol*, *206*(7), 895-908.

Oberbach, A., Bossenz, Y., Lehmann, S., Niebauer, J., Adams, V., Paschke, R., ... & Punkt, K. (2006). Altered fiber distribution and fiber-specific glycolytic and oxidative enzyme activity in skeletal muscle of patients with type 2 diabetes. *Diabetes care*, *29*(4), 895-900.

Pearse, A. G. Everson (Anthony Guy Everson) (1972). *Histochemistry, theoretical and applied / Vol.2* (3rd ed). Churchill Livingstone, London (104 Gloucester Place, W1H 4AE)

Pertseva, M. N., & Shpakov, A. O. (2002). Conservatism of the insulin signaling system in evolution of invertebrate and vertebrate animals. *Journal of Evolutionary Biochemistry and Physiology*, *38*(5), 547-561.

Pette, D., & Staron, R. S. (2000). Myosin isoforms, muscle fiber types, and transitions. *Microscopy research and technique*, *50*(6), 500-509.

Piccirillo, R., Demontis, F., Perrimon, N., & Goldberg, A. L. (2014). Mechanisms of muscle growth and atrophy in mammals and Drosophila. *Developmental Dynamics*, *243*(2), 201-215.

Pietuch, A., Brückner, B. R., & Janshoff, A. (2013). Membrane tension homeostasis of epithelial cells through surface area regulation in response to osmotic stress. *Biochimica et Biophysica Acta (BBA)-Molecular Cell Research*, *1833*(3), 712-722.

Porporato, P. E. (2016). Understanding cachexia as a cancer metabolism syndrome. *Oncogenesis*, *5*(2), e200.

Praul, C. A., Brubaker, K. D., Leach, R. M., & Gay, C. V. (1998). Detection of endogenous biotin-containing proteins in bone and cartilage cells with streptavidin systems. *Biochemical and biophysical research communications*, *247*(2), 312-314.

Reedy, M. C., Bullard, B., & Vigoreaux, J. O. (2000). Flightin is essential for thick filament assembly and sarcomere stability in Drosophila flight muscles. *The Journal of cell biology*, *151*(7), 1483-1500.

Roch-Norlund, A. E., Bergström, J., Castenfors, H., & Hultman, E. (1970). Muscle glycogen in patients with diabetes mellitus. *Journal of Internal Medicine*, *187*(1-6), 445-453.

Sacktor, B. (1955). Cell structure and the metabolism of insect flight muscle. *The Journal of biophysical and biochemical cytology*, *1*(1), 29.

Saitoh, M., Ishida, J., Doehner, W., von Haehling, S., Anker, M. S., Coats, A. J., ... & Springer, J. (2017). Sarcopenia, cachexia, and muscle performance in heart failure: Review update 2016. *International journal of cardiology*, *238*, 5-11.

Sandri, M., Sandri, C., Gilbert, A., Skurk, C., Calabria, E., Picard, A., ... & Goldberg, A. L. (2004). Foxo transcription factors induce the atrophy-related ubiquitin ligase atrogin-1 and cause skeletal muscle atrophy. *Cell*, *117*(3), 399-412.

Sayer, A. A., Dennison, E. M., Syddall, H. E., Gilbody, H. J., Phillips, D. I., & Cooper, C. (2005). Type 2 diabetes, muscle strength, and impaired physical function: the tip of the iceberg?. *Diabetes care*, *28*(10), 2541-2542.

Scott, W., Stevens, J., & Binder–Macleod, S. A. (2001). Human skeletal muscle fiber type classifications. *Physical therapy*, *81*(11), 1810-1816.

Song, X. M., Kawano, Y., Krook, A., Ryder, J. W., Efendic, S., Roth, R. A., ... & Zierath, J. R. (1999). Muscle fiber type-specific defects in insulin signal transduction to glucose transport in diabetic GK rats. *Diabetes*, *48*(3), 664-670.

Stitt, T. N., Drujan, D., Clarke, B. A., Panaro, F., Timofeyva, Y., Kline, W. O., ... & Glass, D. J. (2004). The IGF-1/PI3K/Akt pathway prevents expression of muscle atrophy-induced ubiquitin ligases by inhibiting FOXO transcription factors. *Molecular cell*, *14*(3), 395-403.

Suarez, R. K. (2000). Energy metabolism during insect flight: biochemical design and physiological performance. *Physiological and Biochemical Zoology*, *73*(6), 765-771.

Suster, M. L., Seugnet, L., Bate, M., & Sokolowski, M. B. (2004). Refining GAL4-driven transgene expression in Drosophila with a GAL80 enhancer-trap. *genesis*, *39*(4), 240-245.

Swank, D. M. (2012). Mechanical analysis of Drosophila indirect flight and jump muscles. *Methods*, *56*(1), 69-77.

Teleman, A. A., Chen, Y. W., & Cohen, S. M. (2005). 4E-BP functions as a metabolic brake used under stress conditions but not during normal growth. *Genes & development*, *19*(16), 1844-1848.

Tetreault, M. P., Yang, Y., & Katz, J. P. (2013). Krüppel-like factors in cancer. *Nature Reviews Cancer*, *13*(10), 701.

Tettweiler, G., Miron, M., Jenkins, M., Sonenberg, N., & Lasko, P. F. (2005). Starvation and oxidative stress resistance in Drosophila are mediated through the eIF4E-binding protein, d4E-BP. *Genes & development*, *19*(16), 1840-1843.

Tisdale, M. J. (2002). Cachexia in cancer patients. *Nature Reviews Cancer*, *2*(11), 862.

Tisdale, M. J. (2008). Catabolic mediators of cancer cachexia. *Current opinion in supportive and palliative care*, *2*(4), 256-261.

Trappe, S., Luden, N., Minchev, K., Raue, U., Jemiolo, B., & Trappe, T. A. (2015). Skeletal muscle signature of a champion sprint runner. *Journal of Applied Physiology*, *118*(12), 1460-1466.

Vigoreaux, J. O., Saide, J. D., Valgeirsdottir, K., & Pardue, M. L. (1993). Flightin, a novel myofibrillar protein of Drosophila stretch-activated muscles. *The Journal of cell biology*, *121*(3), 587-598.

Wang, X., & Proud, C. G. (2006). The mTOR pathway in the control of protein synthesis. *Physiology*, *21*(5), 362-369.

Weiss, M., Steiner, D. F., & Philipson, L. H. (2014). Insulin biosynthesis, secretion, structure, and structure-activity relationships.

Wilson, R. C., & Doudna, J. A. (2013). Molecular mechanisms of RNA interference. *Annual review of biophysics*, *42*, 217-239.

Zhang, H., Chen, Q., Yang, M., Zhu, B., Cui, Y., Xue, Y., ... & Zhang, S. (2013). Mouse KLF11 regulates hepatic lipid metabolism. *Journal of hepatology*, *58*(4), 763-770.

Zhou, X., Wang, J. L., Lu, J., Song, Y., Kwak, K. S., Jiao, Q., ... & Lacey, D. L. (2010). Reversal of cancer cachexia and muscle wasting by ActRIIB antagonism leads to prolonged survival. *Cell*, *142*(4), 531-543.

Zid, B. M., Rogers, A. N., Katewa, S. D., Vargas, M. A., Kolipinski, M. C., Lu, T. A., ... & Kapahi, P. (2009). 4E-BP extends lifespan upon dietary restriction by enhancing mitochondrial activity in Drosophila. *Cell*, *139*(1), 149-160.